Annalen der Physik (Berlin) **527** (2015) 663-683

Scattering theory and thermodynamics of quantum transport

Pierre Gaspard
Center for Nonlinear Phenomena and Complex Systems – Department of Physics, Université Libre de Bruxelles, Code Postal 231, Campus Plaine, B-1050 Brussels, Belgium

Scattering theory is complemented by recent results on full counting statistics, the multivariate fluctuation relation for currents, and time asymmetry in temporal disorder characterized by the Connes-Narnhofer-Thirring entropy per unit time, in order to establish relationships with the thermodynamics of quantum transport. Fluctuations in the bosonic or fermionic currents flowing across an open system in contact with particle reservoirs are described by their cumulant generating function, which obeys the multivariate fluctuation relation as the consequence of microreversibility. Time asymmetry in temporal disorder is shown to manifest itself out of equilibrium in the difference between a time-reversed coentropy and the Connes-Narnhofer-Thirring entropy per unit time. This difference is shown to be equal to the thermodynamic entropy production for ideal quantum gases of bosons and fermions. The results are illustrated for a two-terminal circuit.

I. INTRODUCTION

Scattering theory is concerned with the external dynamics of unbounded particles flowing from and to infinity, and having continuous energy spectra [1, 2]. In contrast, the internal dynamics involves the bound states, which form discrete energy spectra and generate quasiperiodic time evolutions. By allowing the formulation of quantum mechanics in systems of infinite spatial extension, scattering theory paves the way to the description of transport properties for open systems in contact with particle and heat reservoirs [3–6]. If the reservoirs have different temperatures and chemical potentials, such open systems are out of equilibrium and they produce thermodynamic entropy. Since Landauer's pioneering work [7], advances have shown how the transport and thermodynamic properties can be rigorously formulated on the basis of scattering theory [8–22]. The great advantage of scattering theory is that the quantum coherence of Hamiltonian microdynamics is preserved during the whole time evolution between the incoming and outgoing paths.

The purpose of the present article is to explain how the time-reversal symmetry of Hamiltonian microdynamics can be compatible with the thermodynamic time asymmetry, notably associated with the breaking of detailed balance in quantum transport. The key issue is that the equations of motion may have solutions that do not share the symmetry of the equations. This phenomenon of symmetry breaking is well known in condensed matter physics and also concerns the time-reversal symmetry. The breaking takes place at the statistical level of description due to the fact that forward and time-reversed paths have different probabilities under nonequilibrium conditions.

These issues are addressed in the framework of large-deviation theory for the transport properties. This theory has been developed since work on dynamical chaos in the eighties [23]. In this context, an analogy has been drawn between spatial disorder studied for long in equilibrium statistical mechanics and temporal disorder, which manifests itself in chaotic systems and stochastic processes. Temporal disorder, alias dynamical randomness, can be characterized by the concept of ϵ-entropy per unit time [24], which reduces to the Kolmogorov-Sinai entropy per unit time in deterministic dynamical systems [25, 26]. The ϵ-entropy per unit time is the rate of information produced by a dynamical system or a stochastic process observed with a spatial or temporal resolution ϵ. The entropy per unit time is vanishing for periodic or quasiperiodic dynamics and positive for chaotic systems or stochastic processes such a Brownian motion. In the eighties also, this concept of entropy per unit time has been generalized to quantum systems by Connes, Narnhofer, and Thirring, allowing us to characterize temporal disorder as well in many-body quantum systems of bosons or fermions [27, 28].

Temporal disorder also manifests itself in open systems sustaining scattering or transport processes, because of the random arrivals of particles coming from remote space or surrounding reservoirs. In this regard, an important issue is to know if its characterization with the Connes-Narnhofer-Thirring entropy per unit time can be extended to open quantum systems under nonequilibrium conditions. For such systems, the breaking of detailed balance results into the time asymmetry of temporal disorder, whereupon relationships can be established between temporal disorder characterized by the aforementioned quantities and thermodynamic entropy production [29–33]. Interestingly, these relationships – which have been anticipated since the nineties by the escape-rate formalism [34–36] – involve the scattering process at the basis of transport.

Moreover, methods have been developed to carry out the full counting statistics of the currents flowing in mesoscopic

electronic circuits since pioneering work by Levitov and Lesovik [10, 11]. These methods are based on large-deviation theory and they extend Landauer's scattering approach from conductance to all the statistical cumulants of the fluctuating currents [6]. Here, the time-reversal symmetry has been shown to have fundamental implications known as the so-called fluctuation relations [14, 20–22, 37–45], as well as generalizations of Onsager's reciprocity relations from the linear to the nonlinear response coefficients [46–53]. These results can be demonstrated for the quantum transport of both bosons and fermions on the basis of scattering theory, as shown here below. This is relevant not only to quantum electron transport in mesoscopic semiconducting devices [3–6], but also to the quantum transport of ultracold atoms [54, 55]. The fluctuation relations describe the breaking of detailed balance away from equilibrium and imply that the entropy production is always non negative in accordance with the second law of thermodynamics.

The presentation of these results is organized as follows. Scattering theory is summarized in Section II. Time-reversal symmetry relations for open quantum systems are introduced in Section III. Quantum transport and its thermodynamics are described for fermions in Section IV and for bosons in Section V. In Section VI, the transport of fermions and bosons is shown to correspond in the classical limit with the well-known kinetic process of effusion. Conclusions are drawn in Section VII.

II. SCATTERING THEORY

A. A few examples of scattering systems

There is a large variety of scattering systems in areas such as particle, nuclear, atomic, molecular, chemical, and mesoscopic physics, photonics, phononics, surface science, gas kinetics, geophysics, astrophysics,... Scattering systems are characterized by unbounded motion before and after collision between particles or with an obstacle. Figure 1 depicts a few examples.

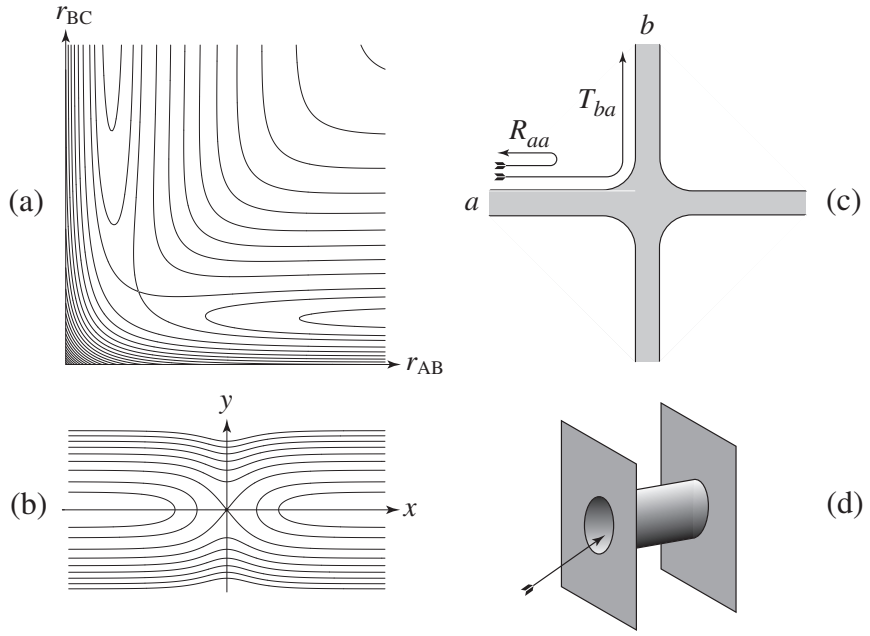

FIG. 1: Examples of scattering systems: (a) Potential energy surface of a collinear reaction A+BC→AB+C in the plane of the distances r_{AB} and r_{BC} between the corresponding atoms. (b) Potential energy surface of a constriction in an electron waveguide in the plane of the axis x of the waveguide and its transverse direction y. (c) Electronic circuit connected with reservoirs by four terminals. (d) Small hole in a wall separating two reservoirs and through which particles undergo effusion.

As shown in Fig. 1a, the potential energy surface of a collinear triatomic system (A, B, C) may present a barrier between two valleys of dissociation [56]. As the distance r_{AB} increases, the atom A moves away from the diatomic molecule BC, which may vibrate while separating from the atom. In the other valley corresponding to $r_{BC} \to \infty$, the atom C separates from the possibly vibrating molecule AB. The three atoms are fully unbounded on the diagonal as $r_{AB} = r_{BC} \to \infty$. Such reactions can be induced between crossed beams of atoms or molecules in a vacuum chamber.

A similar potential energy surface describes the ballistic motion of independent electrons in a semiconducting circuit with a constriction, forming a barrier in a waveguide. In Fig. 1b, the motion is assumed to be harmonic transverse to the axis x of the waveguide and the potential energy is given by $u(x,y) = v_0/(\cosh \alpha x)^2 + m\omega^2 y^2/2$ with a Pöschl-Teller barrier [57]. The waveguide is connected with electron reservoirs on the left- and right-hand sides. If the reservoirs are at different temperatures and chemical potentials, currents are flowing through the waveguide with preferred directions. Some electrons are transmitted while others are scattered by the barrier. Similar potentials apply to ultracold atoms in optical traps with a designed constriction or in magnetic traps on atom chips [54, 55, 58]. Since the particles are conserved together with their energy, particle and heat currents may be coupled together leading, for instance, to thermoelectric effects [9, 54].

Electronic mesoscopic circuits may be connected with more than two reservoirs [3–6, 8]. A circuit with four terminals is schematically depicted in Fig. 1c. In multiterminal circuits with quantum dots and quantum point contacts, the different electronic currents may be coupled by Coulomb drag effects [59–61]. External magnetic fields may induce Hall effects, or Aharonov-Bohm interferences in circuits with loops [3–6].

Transport through a constriction has been investigated long ago [62] in dilute or rarefied gases flowing through a small hole in a wall separating two reservoirs at different pressures and temperatures, as depicted in Fig. 1d. This is the well-known process of effusion, which is described by classical kinetic theory [63, 64]. As shown here below, the results known for effusion can indeed be recovered in the classical limit from the relationships recently established for the quantum transport of bosons and fermions on the basis of scattering theory.

B. Quantum systems with a finite number of particles

At any time t, a quantum system is described by a wave function $\Psi(\mathbf{x},\sigma,t)$ belonging to a Hilbert space of square-integrable functions, $\sum_{\sigma=-s}^{s}\int_{\mathbb{R}^f}|\Psi(\mathbf{x},\sigma,t)|^2 d\mathbf{x} = 1$, where $\mathbf{x}\in\mathbb{R}^f$ denotes the positions and $\sigma = -s, -s+1, ..., s-1, s$ their spin component along some axis of quantization. The time evolution of the wave function is ruled by Schrödinger's equation:

$$i\hbar\partial_t\Psi = \hat{H}\Psi\,, \tag{1}$$

where $i = \sqrt{-1}$, $\hbar$ is Planck's constant, and $\hat{H}$ is the Hamiltonian operator, which is Hermitian [57, 65]. If the Hamiltonian is independent of time, the solution of Schrödinger's equation can be written as

$$\Psi_t = \mathrm{e}^{-\frac{i}{\hbar}\hat{H}t}\Psi_0 \tag{2}$$

in terms of the unitary time-evolution operator. The Hamiltonian operator may have an energy spectrum with a continuous part and possible discrete eigenvalues corresponding to the bound states of particles.

For scattering systems, the Hamiltonian operator $\hat{H}$ reduces at large distances to another one $\hat{H}_0$ describing the asymptotic free motion as

$$\hat{H} = \hat{H}_0 + \hat{V} \qquad \text{with} \quad \hat{V}\to 0 \quad \text{for} \quad \|\mathbf{x}\|\to\infty\,. \tag{3}$$

The asymptotic Hamiltonian has eigenstates, $\hat{H}_0\Phi = E\Phi$, forming a continuous energy spectrum including all the unbounded asymptotic states of the full Hamiltonian. This continuous spectrum may have different branches corresponding to multiple channels. In the space of these unbounded asymptotic states, the scattering operator is defined as [1, 2]

$$\hat{S} \equiv \lim_{t\to\infty} \mathrm{e}^{\frac{i}{\hbar}\hat{H}_0 t/2}\mathrm{e}^{-\frac{i}{\hbar}\hat{H}t}\mathrm{e}^{\frac{i}{\hbar}\hat{H}_0 t/2}\,. \tag{4}$$

This operator can be decomposed onto the energy eigenspaces of the asymptotic Hamiltonian $\hat{H}_0$ as

$$\hat{S} = \int_0^\infty dE\,\hat{S}(E)\,\delta(E-\hat{H}_0)\,, \tag{5}$$

in terms of the scattering matrix $\hat{S}(E)$, which maps incoming asymptotic states onto the outgoing ones:

$$\Phi_{\mathrm{out}} = \hat{S}(E)\,\Phi_{\mathrm{in}}\,. \tag{6}$$

The scattering matrix is unitary

$$\hat{S}^\dagger(E)\hat{S}(E) = \hat{S}(E)\hat{S}^\dagger(E) = \hat{1}\,, \tag{7}$$

and can be expressed as

$$\hat{S}(E) = \hat{1} - 2\pi i\, \delta(E - \hat{H}_0)\, \hat{T}(E + i0) = \hat{T}^{-1}(E - i0)\, \hat{T}(E + i0) \tag{8}$$

in terms of the T-matrix defined as

$$\hat{T}(z) \equiv \hat{V} + \hat{V}\, \frac{1}{z - \hat{H}}\, \hat{V}\,. \tag{9}$$

Equations (8) and (9) show that the scattering matrix admits singularities corresponding to those of the resolvent operator $1/(z - \hat{H})$ for the full Hamiltonian $\hat{H}$ if the energy z is continued towards complex values. In particular, the scattering matrix has poles at the negative energy eigenvalues $\{E_b\}$ of the bound states, branch cuts along the positive energy axis, and poles at complex energies $\{E_r\}$ corresponding to resonances with $\mathrm{Im}\, E_r < 0$ and anti-resonances with $\mathrm{Im}\, E_r > 0$. Every branch cut extends over $E_c^0 \leq E < +\infty$ from the energy threshold E_c^0 where the channel c starts to be open. The continuous spectrum can be characterized by an excess level density relative to free motion:

$$D(E) \equiv \mathrm{tr}\, \left[\delta(E - \hat{H}) - \delta(E - \hat{H}_0)\right]\,. \tag{10}$$

This excess level density is related to Wigner's time delay [66] by

$$\mathcal{T}(E) \equiv \frac{\hbar}{i}\, \mathrm{tr}\, \frac{d}{dE}\, \ln \hat{S}(E) = 2\pi\hbar\, D(E)\,, \tag{11}$$

which measures the delay in the wave propagation at the energy E due to interaction with the scatterer.

C. Semiclassics and the classical limit

Wave propagation can be described using Feynman's path integrals. In the limit where the path actions are larger than Planck's constant

$$W = \int \mathbf{p} \cdot d\mathbf{x} - H dt \gg \hbar\,, \tag{12}$$

path integrals are dominated by the classical trajectories, which are solutions of Hamilton's equations:

$$\begin{cases} \dot{\mathbf{x}} = \dfrac{\partial H_{\mathrm{cl}}}{\partial \mathbf{p}}\,, \\ \\ \dot{\mathbf{p}} = -\dfrac{\partial H_{\mathrm{cl}}}{\partial \mathbf{x}}\,, \end{cases} \tag{13}$$

where $H_{\mathrm{cl}}(\mathbf{x}, \mathbf{p})$ is the Hamiltonian function corresponding to the Hamiltonian operator $\hat{H}$ and $\mathbf{p} \in \mathbb{R}^f$ are the momenta canonically conjugated to the positions $\mathbf{x} \in \mathbb{R}^f$. If the Hamiltonian is independent of time, a flow of trajectories $\mathbf{\Phi}^t$ is defined in the phase space $\mathbf{\Gamma} = (\mathbf{x}, \mathbf{p}) \in \mathbb{R}^{2f}$.

For a scattering system, the Hamiltonian function can again be decomposed as $H_{\mathrm{cl}} = H_{0,\mathrm{cl}} + V_{\mathrm{cl}}$ into an asymptotic one $H_{0,\mathrm{cl}}$ describing asymptotic free motion and an interaction V_{cl} with the scatterer. In analogy with Eq. (4), a scattering function can be defined as [67]

$$\mathbf{\Sigma} \equiv \lim_{t \to \infty} \mathbf{\Phi}_0^{-t/2} \circ \mathbf{\Phi}^t \circ \mathbf{\Phi}_0^{-t/2}\,, \tag{14}$$

which maps the incoming trajectories onto the outgoing ones:

$$\mathbf{\Gamma}_{\mathrm{out}} = \mathbf{\Sigma}(\mathbf{\Gamma}_{\mathrm{in}})\,. \tag{15}$$

If there exist trajectories that are trapped forever in or close to the scatterer and if these trajectories are all unstable, the excess level density (10) can be approximated as [68]

$$D(E) = D_{\mathrm{av}}(E) - \frac{1}{\pi}\, \frac{d}{dE}\, \ln Z_{\mathrm{sc}}(E) + O(\hbar^0)\,, \tag{16}$$

in terms of the average excess level density

$$D_{\rm av}(E) = \int \frac{d\mathbf{x}\, d\mathbf{p}}{(2\pi\hbar)^f} \, \{\delta\left[E - H_{\rm cl}(\mathbf{x},\mathbf{p})\right] - \delta\left[E - H_{0,\rm cl}(\mathbf{x},\mathbf{p})\right]\} + O(\hbar^{-f+1}) \,, \tag{17}$$

and the Gutzwiller-Voros zeta function [69, 70] given by

$$Z_{\rm sc}(E) = \prod_{m=0}^{\infty} \prod_{p} \left(1 - \frac{\mathrm{e}^{\frac{i}{\hbar} S_p - i\frac{\pi}{2}\mu_p}}{|\Lambda_p|^{1/2} \Lambda_p^m} \right) \,, \tag{18}$$

for systems with two degrees of freedom $f = 2$. The zeta function is expressed as a product over the unstable and isolated periodic orbits $\{p\}$ contained among the trapped trajectories and over the integer $m \in \mathbb{N}$. Each periodic orbit is characterized by its reduced action $S_p(E) = \oint_p \mathbf{p}\cdot d\mathbf{x}$, its Maslov index μ_p, and the leading eigenvalue $|\Lambda_p(E)| > 1$ of the linearized Poincaré map of the flow in its vicinity. In this semiclassical approximation, the scattering resonances are given by the zeroes at complex energies $\{E_r\}$ of the Gutzwiller-Voros zeta function. The imaginary part of the complex energy E_r gives the lifetime of the resonances as

$$\tau_r = -\frac{\hbar}{2\,\mathrm{Im}\, E_r} \,. \tag{19}$$

In classically chaotic scatterers such as the three-disk billiard, the quantum lifetimes may be longer than the classical lifetime given by the leading Pollicott-Ruelle resonance of the classical Liouvillian dynamics [71–73]. The chaotic lengthening of quantum lifetimes is due to wave interference between the multiple paths of the classically chaotic dynamics [74]. This phenomenon is reminiscent of Anderson's localization in disordered media. If the scatterer is filamentary enough, the quantum lifetimes may be bounded from above, because a gap is formed in the resonance spectrum. These features have been studied in the three- and four-disk billiards [75–78], in triatomic molecular systems with potential energy surfaces as in Fig. 1a [56], or in quantum graphs [79]. In these systems, the resonance spectrum controls the decay rates, which characterize, in particular, the unimolecular reactions. The time evolution of such systems is transient, but may last long enough to manifest a rich dynamics.

If the number of open channels is large, the fine structure of the scattering matrix may be described using random matrix theory. Different statistical ensembles can be used depending on the fundamental symmetries of the problem under study [80]. These random-matrix properties are the manifestation of the complexity of the scattering dynamics and of the multiplication of quantum states to be considered in the classical limit.

D. Many-body quantum systems

In open systems connected with reservoirs, particles are continuously incoming and outgoing so that a stationary flow can be sustained. Such systems involve an arbitrarily large number of particles and should be described as many-body quantum systems [81]. This is the case for the transport of electrons in mesoscopic circuits or ultracold atoms in optical traps with a constriction. Here, the scatterer is constituted by the cavity or the obstacle between the source and the drain. The scattering region may be in contact with more than two reservoirs in multiterminal circuits.

If the particles are independent of each other, the many-body Hamiltonian operator may be written as

$$\hat{H} = \sum_{\sigma=-s}^{+s} \int d\mathbf{x}\, \hat{\psi}^\dagger(\mathbf{x},\sigma)\, \hat{h}\, \hat{\psi}(\mathbf{x},\sigma) \tag{20}$$

with the one-body Hamiltonian operator:

$$\hat{h} = -\frac{\hbar^2}{2m} \boldsymbol{\nabla}^2 + u(\mathbf{x}) \,, \tag{21}$$

for particles of mass m and spin s. The field operators obey canonical commuting or anticommuting relations

$$\hat{\psi}(\mathbf{x},\sigma)\, \hat{\psi}^\dagger(\mathbf{x}',\sigma') - \theta\, \hat{\psi}^\dagger(\mathbf{x}',\sigma')\, \hat{\psi}(\mathbf{x},\sigma) = \delta(\mathbf{x}-\mathbf{x}')\, \delta_{\sigma\sigma'} \,, \tag{22}$$

whether the particles are bosons if their spin is integral and $\theta = +1$, or fermions if their spin is half-integral and $\theta = -1$. Besides, other observables can be introduced such as the particle density

$$\hat{n}(\mathbf{x}) = \sum_{\sigma=-s}^{+s} \hat{\psi}^\dagger(\mathbf{x},\sigma)\, \hat{\psi}(\mathbf{x},\sigma) \,. \tag{23}$$

The total number of particles is thus given by

$$\hat{N} = \int d\mathbf{x}\, \hat{n}(\mathbf{x})\,, \tag{24}$$

by integrating over the whole space $\mathbf{x} \in \mathbb{R}^3$. The number of particles in some reservoir is defined by restricting the integral to the region of this reservoir. The energy in the reservoirs can be similarly defined in terms of an energy density.

The potential energy $u(\mathbf{r})$ describes the shape of the conducting circuit or optical trap [5, 55]. As shown in Fig. 1b and Fig. 1c, the circuit may have several terminals of infinite spatial extension. In every terminal $l = 1, 2, ..., r$, there exist a spatial coordinate $x_\parallel$ parallel to the axis of the wire and other coordinates $\mathbf{x}_\perp$ transverse to it. Asymptotically for $x_\parallel \to \infty$, the potential energy may be supposed to be independent of the longitudinal coordinate $x_\parallel$:

$$u(\mathbf{x}) \simeq_{x_\parallel \to \infty} u_l(\mathbf{x}_\perp)\,, \tag{25}$$

where $u_l(\mathbf{x}_\perp)$ is the profile of the potential transverse to the wire. This is the case for the potential energy surface of Fig. 1b given by a harmonic potential in the transverse direction $y = x_\perp$ and a Pöschl-Teller barrier [57] describing a constriction in the longitudinal direction $x = x_\parallel$:

$$u(x, y) = \frac{v_0}{(\cosh \alpha x)^2} + \frac{1}{2} m\omega^2 y^2\,. \tag{26}$$

Asymptotically in the wire, the one-body Hamiltonian operator admits stationary states

$$\left[-\frac{\hbar^2}{2m}\nabla^2 + u_l(\mathbf{x}_\perp)\right] \phi = \varepsilon\, \phi \tag{27}$$

of the following form:

$$\phi(\mathbf{x}, \sigma) = \exp\left(\frac{i}{\hbar}\, p\, x_\parallel\right)\, \varphi_{l\mathbf{n}}(\mathbf{x}_\perp)\, \chi_\varsigma(\sigma)\,, \tag{28}$$

where p is the momentum in the direction of the wire l, $\mathbf{n}$ are quantum numbers labeling the transverse modes, and $\chi_\varsigma(\sigma)$ is a spinor with $\varsigma, \sigma = -s, -s+1, ..., s-1, s$. The transverse modes correspond to the different possible channels for transport [6]. The corresponding energy eigenvalues are given by

$$\varepsilon = \varepsilon_{0l\mathbf{n}} + \frac{p^2}{2m}\,. \tag{29}$$

The channel $a = l\mathbf{n}$ is open at energies larger than the threshold $\varepsilon_{0l\mathbf{n}}$. For the potential (26), the thresholds are given by $\varepsilon_{0n} = \hbar\omega(n + 1/2)$ with $n = 0, 1, 2, ...$ Another example is shown in Fig. 2 for a wire with a square cross-section. Figure 2a depicts the dispersion relations (29) and Fig. 2b the number of channels that are open as the energy increases.

Accordingly, the one-body Hamiltonian can be decomposed as $\hat{h} = \hat{h}_0 + \hat{v}$ into an asymptotic Hamiltonian $\hat{h}_0$ given by Eq. (27) and an interaction $\hat{v}$ describing the presence of the scatterer. In the example of the potential (26), the asymptotic Hamiltonian is given by $\hat{h}_0 = -\hbar^2(\partial_x^2 + \partial_y^2)/(2m) + m\omega^2 y^2/2$ and the interaction by $\hat{v} = v_0/(\cosh \alpha x)^2$. The propagation modes in the wires are scattered by the barrier. If the incoming wavefunction is a plane wave in the positive x-direction, the scattering produces the reflected and transmitted waves:

$$\psi_{pn}(x, \sigma) = \begin{cases} \left(\mathrm{e}^{ipx/\hbar} + r_{pn}\, \mathrm{e}^{-ipx/\hbar}\right)\, \varphi_n(y)\, \chi_\varsigma(\sigma) & \text{for} \quad x < 0\,, \\ t_{pn}\, \mathrm{e}^{ipx/\hbar}\, \varphi_n(y)\, \chi_\varsigma(\sigma) & \text{for} \quad x > 0\,, \end{cases} \tag{30}$$

where r_{pn} and t_{pn} denote the reflection and transmission amplitudes depending on the momentum $p = p_x$ and the quantum number $n = 0, 1, 2, ...$ In every channel n, the scattering matrix (6) can be expressed as

$$\hat{S}(\varepsilon) = \begin{pmatrix} r_{pn} & t_{pn} \\ t_{pn} & r_{pn} \end{pmatrix}\,, \tag{31}$$

in terms of the one-body energy $\varepsilon = \varepsilon_{0n} + p^2/(2m)$ [6]. The transmission probability through the barrier is thus given by $T_n(\varepsilon) = |t_{pn}|^2$ and the reflection probability by $R_n(\varepsilon) = |r_{pn}|^2 = 1 - T_n(\varepsilon)$. The scattering matrix is 2×2 because the energy potential is separable in the $x_\parallel$ and $\mathbf{x}_\perp$ directions. In this case, the transmission coefficient can be written

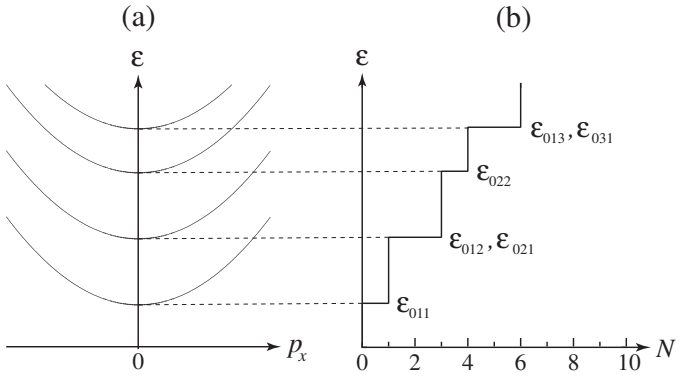

FIG. 2: (a) Energy spectrum in a waveguide with hard walls separated by the distance ℓ in the transverse y- and z-directions versus the momentum $p = p_x$ in the x-direction $\varepsilon = \varepsilon_{0n_yn_z} + p_x^2/(2m)$ with $\varepsilon_{0n_yn_z} = (\pi\hbar/\ell)^2 (n_y^2 + n_z^2)/(2m)$ for $n_y, n_z = 1, 2, 3, ...$ (b) Corresponding diagram showing the number N of open channels as the one-body energy increases (vertical axis).

as $T_n(\varepsilon) = T(\varepsilon - \varepsilon_{0\mathbf{n}})$ in terms of the transmission coefficient $T(\varepsilon)$ of the one-dimensional barrier $v(x)$. Examples of such transmission probabilities are depicted in Fig. 3. The transmission probability converges to the unit value at high energy well above the height of the barrier. For energies lower than the height of the barrier, the transmission proceeds by tunneling. The broader the barrier, the smaller the transmission probability. For the inverted parabolic potential $v(x) = v_0 - m\gamma^2 x^2/2$, the transmission probability is given by [82]

$$T(\varepsilon) = \left[1 + \exp\left(-2\pi \frac{\varepsilon - v_0}{\hbar\gamma}\right)\right]^{-1} . \tag{32}$$

Since the potential is unbounded below, the transmission probability remains positive for $\varepsilon \leq 0$ and vanishes only in the limit $\varepsilon \to -\infty$, as shown in Fig. 3c. For the three other potentials, which are vanishing at large distances, the transmission probability is strictly equal to zero for $\varepsilon \leq 0$.

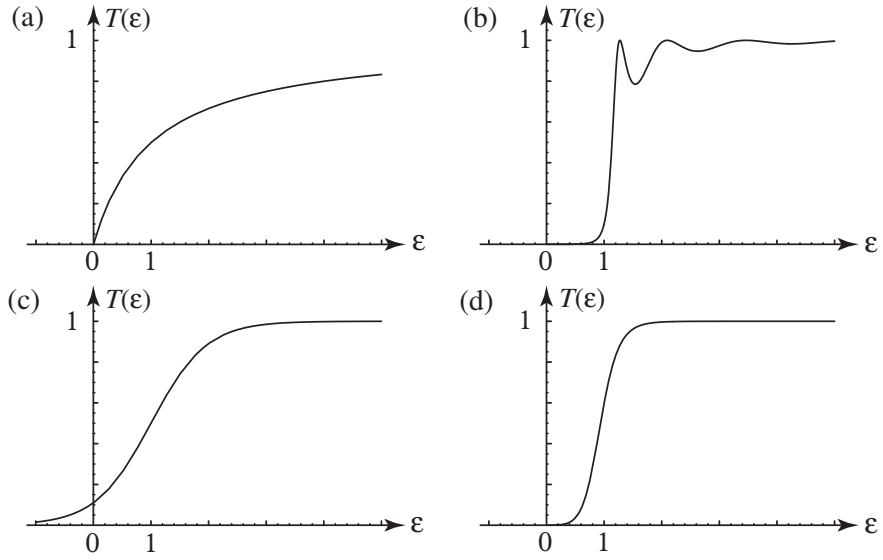

FIG. 3: The transmission probability $T(\varepsilon)$ versus the energy ε for different types of barriers: (a) the delta barrier $v(x) = g\,\delta(x)$ with $g = 2$ [65]; (b) the square barrier of height $v_0 = 1$ and width $\ell = 6$ [57, 65]; (c) the inverted parabolic barrier $v(x) = v_0 - m\gamma^2 x^2/2$ with $v_0 = 1$ and $\gamma = 3$ [82]; (d) the Pöschl-Teller barrier $v(x) = v_0/(\cosh \alpha x)^2$ with $v_0 = 1$ and $\alpha = 1/2$ [57]. For every barrier, the mass is $m = 1/2$ and $\hbar = 1$.

For non-separable potentials, the scattering matrix is infinite and couples together the transverse modes [83, 84].

III. TIME-REVERSAL SYMMETRY RELATIONS FOR OPEN QUANTUM SYSTEMS

A. Multivariate fluctuation relation for currents

1. General open quantum systems

In open quantum systems connected with reservoirs of particles, an important problem is to count energy and particles that are exchanged between the reservoirs during some time interval $[0,t]$. Beyond the mean currents, the counting statistics can be carried out in order to characterize the current fluctuations thanks to their diffusivities or higher cumulants [6, 10, 11]. All these quantities can be deduced from the so-called cumulant generating function, which captures the large-deviation properties of the current fluctuations. These properties can be investigated close or far from equilibrium, depending on the biases imposed between the reservoirs.

Recent work has shown that the cumulant generating function obeys a remarkable symmetry as the consequence of microreversibility [20–22, 46–53]. This symmetry known as the multivariate fluctuation relation for currents has fundamental implications on the linear and nonlinear response coefficients of the open system. In particular, the Green-Kubo formulae and Onsager reciprocity relations can be generalized from the linear to the nonlinear response coefficients [46–48, 50, 51]. The purpose of this subsection is to show that these results can be established systematically for open systems of independent bosons or fermions thanks to the scattering approach.

The counting statistics of the energy and particles exchanged between the reservoirs can be carried out in a scheme with the preparation of initial states and the measurement of final outcomes [50], as it is also the case in scattering theory. The reservoirs $l = 1, 2, ..., r$ are assumed to be non interacting for times $\tau < 0$ and $t < \tau$. The interaction is switched on during the time interval $[0,t]$. If $\hat{H}_l$ denotes the Hamiltonian operator of the $l^{\rm th}$ reservoir and $\hat{N}_l$ the number of particles in this reservoir, the total Hamiltonian and total particle-number operators are given by

$$\hat{H} \;=\; \sum_{l=1}^{r} \hat{H}_l + \hat{V}\,, \tag{33}$$

$$\hat{N} \;=\; \sum_{l=1}^{r} \hat{N}_l\,, \tag{34}$$

where $\hat{V}$ is the interaction energy, which is vanishing for $\tau < 0$ and $t < \tau$ [44, 50]. The reservoir operators commute with each other: $[\hat{H}_l, \hat{H}_{l'}] = [\hat{H}_l, \hat{N}_{l'}] = [\hat{N}_l, \hat{N}_{l'}] = 0$ for $l, l' = 1, 2, ..., r$. These operators are symmetric under time reversal, which is represented by the antiunitary operator $\hat{\Theta}$. In particular, microreversibility is expressed by the time-reversal symmetry of the total Hamiltonian ruling time evolution:

$$\hat{\Theta}\,\hat{H} = \hat{H}\,\hat{\Theta}\,. \tag{35}$$

Initially, the system is supposed to be in a grand-canonical statistical ensemble at the temperatures $\{T_l\}_{l=1}^r$ and chemical potentials $\{\mu_l\}_{l=1}^r$ of the reservoirs:

$$\hat{\rho}(0) = \prod_{l=1}^{r} \frac{1}{\Xi_l}\, {\rm e}^{-\beta_l(\hat{H}_l - \mu_l \hat{N}_l)}\,, \tag{36}$$

with the inverse temperatures $\beta_l = (k_{\rm B}T_l)^{-1}$ and Boltzmann's constant $k_{\rm B}$. The grand-canonical thermodynamic potential of the $l^{\rm th}$ reservoir is defined as $\Phi_l = -k_{\rm B}T_l \ln \Xi_l$ in terms of the corresponding partition function.

During the semi-infinite lapse of time $\tau < 0$, a quantum measurement is performed in order to determine the initial values $\{E_{li}, N_{li}\}$ of the energies and particle numbers in all the decoupled reservoirs:

$$\tau < 0: \qquad \left\{ \begin{array}{l} \hat{H}_l\,|\Psi_i\rangle = E_{li}\,|\Psi_i\rangle \\ \hat{N}_l\,|\Psi_i\rangle = N_{li}\,|\Psi_i\rangle \end{array} \right. \qquad \forall\; l = 1, 2, ..., r\,, \tag{37}$$

where $|\Psi_i\rangle$ is thus the initial state of probability

$$\langle\Psi_i|\hat{\rho}(0)|\Psi_i\rangle = \prod_{l=1}^{r} {\rm e}^{-\beta_l(\hat{E}_{li} - \mu_l N_{li} - \Phi_l)}\,. \tag{38}$$

After the time interval $[0,t]$ when the reservoirs are again decoupled, another quantum measurement is performed over the semi-infinite lapse of time $t < \tau$ to get the final values $\{E_{lf}, N_{lf}\}$ of the energies and particle numbers in the

reservoirs:

$$t < \tau : \qquad \left\{ \begin{array}{l} \hat{H}_l \, |\Psi_f\rangle = E_{lf} \, |\Psi_f\rangle \\ \hat{N}_l \, |\Psi_f\rangle = N_{lf} \, |\Psi_f\rangle \end{array} \right. \qquad \forall \; l = 1, 2, ..., r \, , \tag{39}$$

for the final state $|\Psi_f\rangle$ happening with the conditional probability

$$|\langle \Psi_f | \hat{U}(t) | \Psi_i \rangle|^2 \tag{40}$$

given in terms of the evolution operator

$$\hat{U}(t) = \mathrm{e}^{-i\hat{H}t/\hbar} \qquad \text{such that} \qquad \hat{\Theta} \, \hat{U}(t) = \hat{U}^\dagger(t) \, \hat{\Theta} = \hat{U}(-t) \, \hat{\Theta} \, . \tag{41}$$

If the initial and final states are observed to be $|\Psi_i\rangle$ and $|\Psi_f\rangle$, the energies and particle numbers in the reservoirs are changing by

$$\left\{ \begin{array}{l} \Delta E_l = E_{lf} - E_{li} \\ \Delta N_l = N_{lf} - N_{li} \end{array} \right. \qquad \forall \; l = 1, 2, ..., r \, . \tag{42}$$

Therefore, the probability density to observe the changes $\Delta \mathbf{E} = \{\Delta E_l\}_{l=1}^r$ and $\Delta \mathbf{N} = \{\Delta N_l\}_{l=1}^r$ in the reservoirs is found to be

$$p_t(\Delta \mathbf{E}, \Delta \mathbf{N}) = \sum_{fi} \langle \Psi_i | \hat{\rho}(0) | \Psi_i \rangle \, |\langle \Psi_f | \hat{U}(t) | \Psi_i \rangle|^2 \, \prod_{l=1}^r \delta(\Delta E_l - E_{lf} + E_{li}) \, \delta(\Delta N_l - N_{lf} + N_{li}) \, . \tag{43}$$

Because of the time-reversal symmetry, this probability density obeys the relation

$$p_t(\Delta \mathbf{E}, \Delta \mathbf{N}) = \mathrm{e}^{\sum_{l=1}^r \beta_l (\Delta E_l - \mu_l \Delta N_l)} \, p_t(-\Delta \mathbf{E}, -\Delta \mathbf{N}) \, , \tag{44}$$

which is not yet the relation we are looking for because it only concerns the changes of energies and particle numbers in the reservoirs during a finite time interval $[0, t]$.

Instead, we are looking for a relation about the exchanges of energy and particle numbers from the reservoirs $l = 1, 2, ..., r-1$ toward a reference reservoir $l = r$ [50]. Indeed, the open system is driven in a nonequilibrium steady state by different temperatures and chemical potentials between $r-1$ reservoirs and some reference reservoir, which may be taken as the r^{th} one. These differences define the so-called affinities or thermodynamic forces:

$$\text{thermal affinities:} \qquad A_{lE} \equiv \beta_r - \beta_l \, , \tag{45}$$

$$\text{chemical affinities:} \qquad A_{lN} \equiv \beta_l \, \mu_l - \beta_r \, \mu_r \, , \tag{46}$$

with $l = 1, 2, ..., r-1$ [85–89]. The steady state is expected to be reached in the long-time limit $t \to \infty$. The equilibrium state corresponds to the steady state with vanishing affinities: $\mathbf{A} = 0$.

With this aim, we introduce the moment generating function

$$G_t(\boldsymbol{\lambda}) \equiv \int \prod_{l=1}^r d\Delta E_l \, d\Delta N_l \, \mathrm{e}^{\sum_{l=1}^{r-1} (\lambda_{lE} \Delta E_l + \lambda_{lN} \Delta N_l)} \, p_t(\Delta \mathbf{E}, \Delta \mathbf{N}) \, , \tag{47}$$

in terms of the $2r-2$ counting parameters $\boldsymbol{\lambda} = \{\lambda_{lE}, \lambda_{lN}\}_{l=1}^{r-1}$. The counting parameters of the r^{th} reservoir are set equal to zero: $\lambda_{rE} = \lambda_{rN} = 0$. A statistical moment of any order can be obtained by taking the required derivatives with respect to these parameters. The cumulant generating function is defined as

$$Q_{\mathbf{A}}(\boldsymbol{\lambda}) \equiv \lim_{t \to \infty} -\frac{1}{t} \, \ln G_t(\boldsymbol{\lambda}) \, , \tag{48}$$

which characterizes a steady state corresponding to the affinities $\mathbf{A} = \{A_{lE}, A_{lN}\}_{l=1}^{r-1}$ since the infinite-time limit is here taken. The statistical cumulants are given by successive derivatives with respect to the counting parameters. In particular, the mean energy and particle currents from the l^{th} reservoir are given by

$$\langle J_{lE} \rangle_{\mathbf{A}} \; = \; \frac{\partial Q_{\mathbf{A}}}{\partial \lambda_{lE}}(\mathbf{0}) = \lim_{t \to \infty} -\frac{1}{t} \, \langle \Delta E_l \rangle_{\mathbf{A}} \, , \tag{49}$$

$$\langle J_{lN} \rangle_{\mathbf{A}} \; = \; \frac{\partial Q_{\mathbf{A}}}{\partial \lambda_{lN}}(\mathbf{0}) = \lim_{t \to \infty} -\frac{1}{t} \, \langle \Delta N_l \rangle_{\mathbf{A}} \, , \tag{50}$$

for $l = 1, 2, ..., r-1$. Beyond, higher cumulants are obtained such as the current diffusivities in the steady state. Since the system is in a steady state, energy and particle conservations imply that

$$\langle J_{rE}\rangle_{\mathbf{A}} = -\sum_{l=1}^{r-1}\langle J_{lE}\rangle_{\mathbf{A}}\,, \tag{51}$$

$$\langle J_{rN}\rangle_{\mathbf{A}} = -\sum_{l=1}^{r-1}\langle J_{lN}\rangle_{\mathbf{A}}\,. \tag{52}$$

Over the long-time interval needed to reach such a steady state, we may assume that energy and particles are also conserved so that the changes of energy and particle number in the reference reservoir are given by $\Delta E_r \simeq -\sum_{l=1}^{r-1}\Delta E_l$ and $\Delta N_r \simeq -\sum_{l=1}^{r-1}\Delta N_l$ [43]. With this assumption, the moment generating function (47) can be transformed using the symmetry relation (44) to get: $G_t(\boldsymbol{\lambda}) \simeq G_t(\mathbf{A}-\boldsymbol{\lambda})$. Accordingly, the cumulant generating function (48) obeys the *multivariate fluctuation relation for currents*:

$$Q_{\mathbf{A}}(\boldsymbol{\lambda}) = Q_{\mathbf{A}}(\mathbf{A}-\boldsymbol{\lambda}) \tag{53}$$

as the consequence of microreversibility [50]. The aforementioned assumption is non trivial to justify, which was done in Ref. [50] for general open quantum systems. This assumption can also be justified for independent particles using scattering theory, as shown in Ref. [51] (see below).

Since the cumulants are obtained by taking derivatives of the generating function (48) with respect to the counting parameters, the multivariate fluctuation relation (53) implies symmetry relations for cumulants of every order [46–48]. As a consequence, the Green-Kubo formulae and the Onsager reciprocity relations are recovered between the linear response coefficients and the diffusivities at equilibrium. Furthermore, generalizations of these fundamental properties are deduced between the nonlinear response coefficients, higher cumulants, and the responses of higher cumulants around equilibrium [46–48]. In the presence of an external magnetic field, generalizations of the Casimir-Onsager reciprocity relations can be inferred as well [50, 51, 53].

2. Open quantum systems with independent particles

For independent particles, the Hamiltonian and other observables are quadratic functions of the annihilation and creation operators $\{\hat{a}_\nu, \hat{a}_\nu^\dagger\}$ of a particle in one-body states $\{\phi_\nu\}$:

$$\hat{X} = \sum_{\nu,\nu'} x_{\nu\nu'}\,\hat{a}_\nu^\dagger\,\hat{a}_{\nu'} = \Gamma(\hat{x})\,, \tag{54}$$

where $\hat{X}$ denotes the many-body operator and $\hat{x} = (x_{\nu\nu'})$ the corresponding one-body operator. The annihilation and creation operators obey the commuting or anticommuting relations:

$$\hat{a}_\nu\,\hat{a}_{\nu'}^\dagger - \theta\,\hat{a}_{\nu'}^\dagger\,\hat{a}_{\nu'} = \delta_{\nu\nu'}\,, \tag{55}$$

whether the particles are bosons ($\theta = +1$) or fermions ($\theta = -1$). Klich has shown that the trace of the products of two exponential functions of many-body operators (54) can be expressed as an appropriate determinant of the corresponding one-body operators [22, 90, 91]:

$$\mathrm{Tr}\,\mathrm{e}^{\hat{X}}\,\mathrm{e}^{\hat{Y}} = \mathrm{Tr}\,\mathrm{e}^{\Gamma(\hat{x})}\,\mathrm{e}^{\Gamma(\hat{y})} = \det\left(1-\theta\,\mathrm{e}^{\hat{x}}\,\mathrm{e}^{\hat{y}}\right)^{-\theta}. \tag{56}$$

Now, the moment generating function (47) can be written as

$$G_t(\boldsymbol{\lambda}) = \mathrm{Tr}\,\hat{\rho}(0)\,\mathrm{e}^{i\hat{H}t/\hbar}\,\mathrm{e}^{\sum_{l=1}^{r-1}(\lambda_{lE}\hat{H}_l+\lambda_{lN}\hat{N}_l)}\,\mathrm{e}^{-i\hat{H}t/\hbar}\,\mathrm{e}^{-\sum_{l=1}^{r-1}(\lambda_{lE}\hat{H}_l+\lambda_{lN}\hat{N}_l)}\,, \tag{57}$$

in terms of the initial density matrix (36), the total Hamiltonian $\hat{H}$, the Hamiltonian and particle-number operators $\{\hat{H}_l, \hat{N}_l\}$ of the reservoirs, and the counting parameters $\{\lambda_{lE}, \lambda_{lN}\}$. Accordingly, the moment generating function takes the form

$$G_t(\boldsymbol{\lambda}) = \frac{\mathrm{Tr}\,\mathrm{e}^{\hat{Y}_t}\,\mathrm{e}^{-\hat{X}-\hat{Y}}}{\mathrm{Tr}\,\mathrm{e}^{-\hat{X}}} \tag{58}$$

with the commuting operators

$$\hat{X} = \sum_{l=1}^{r} \beta_l (\hat{H}_l - \mu_l \hat{N}_l) \,, \tag{59}$$

$$\hat{Y} = \sum_{l=1}^{r-1} (\lambda_{lE} \hat{H}_l + \lambda_{lN} \hat{N}_l) \,, \tag{60}$$

and $\hat{Y}_t = \mathrm{e}^{i\hat{H}t/\hbar}\, \hat{Y}\, \mathrm{e}^{-i\hat{H}t/\hbar}$. Introducing the Bose-Einstein and Fermi-Dirac distribution functions of all the reservoirs as

$$\hat{f} = \frac{1}{\mathrm{e}^{\hat{x}} - \theta} = \frac{1}{\mathrm{e}^{\sum_{l=1}^{r} \beta_l (\hat{h}_l - \mu_l \hat{n}_l)} - \theta} \,, \tag{61}$$

Klich's formula (56) transforms the moment generating function into

$$G_t(\boldsymbol{\lambda}) = \det \left[1 - \theta \hat{f} \left(\mathrm{e}^{\hat{y}_t}\, \mathrm{e}^{-\hat{y}} - 1 \right) \right]^{-\theta} \,. \tag{62}$$

Considering a long but finite time interval $[0, t]$, the time evolution can be expressed in terms of the scattering operator (4) as

$$\mathrm{e}^{\hat{y}_t} = \mathrm{e}^{i\hat{h}t}\, \mathrm{e}^{\hat{y}}\, \mathrm{e}^{-i\hat{h}t} \simeq \mathrm{e}^{i\hat{h}_0 t/2}\, \hat{S}^\dagger\, \mathrm{e}^{\hat{y}}\, \hat{S}\, \mathrm{e}^{-i\hat{h}_0 t/2} \qquad \text{for} \quad t \to \infty \,, \tag{63}$$

here for the one-body dynamics with the asymptotic non-interacting Hamiltonian $\hat{h}_0 = \sum_{l=1}^{r} \hat{h}_l$ and $\hbar = 1$. Since $\hat{h}_0$ commutes with $\hat{f}$ and $\hat{y}$, the moment generating function becomes [90]:

$$G_t(\boldsymbol{\lambda}) \simeq \det \left[1 - \theta \hat{f} \left(\hat{S}^\dagger\, \mathrm{e}^{\hat{y}}\, \hat{S}\, \mathrm{e}^{-\hat{y}} - 1 \right) \right]^{-\theta} \,. \tag{64}$$

In principle, the determinant is taken in the Hilbert space of the one-body dynamics, but the finite time interval constrains the one-body energy spectrum to be discrete with a spacing equal to

$$\Delta\varepsilon = \frac{2\pi\hbar}{t} \,, \tag{65}$$

such that the energy spectrum forms a quasicontinuum in the long-time limit:

$$\lim_{t\to\infty} \frac{1}{t} \sum_{\varepsilon,\sigma} (\cdot) = g_s \int \frac{d\varepsilon}{2\pi\hbar} \, (\cdot) \,, \tag{66}$$

where the sum extends over the discrete energy and spin states with $\sigma = -s, -s+1, ..., s-1, s$ and $g_s = 2s+1$ [92]. Decomposing the one-body operators over energy as in Eq. (5) for the scattering operator, the moment generating function can thus be written as

$$G_t(\boldsymbol{\lambda}) \simeq \prod_{\varepsilon,\sigma} \det \left\{ 1 - \theta \hat{f}(\varepsilon) \left[\hat{S}^\dagger(\varepsilon)\, \mathrm{e}^{\varepsilon \hat{\lambda}_E + \hat{\lambda}_N}\, \hat{S}(\varepsilon)\, \mathrm{e}^{-\varepsilon \hat{\lambda}_E - \hat{\lambda}_N} - 1 \right] \right\}^{-\theta} \,. \tag{67}$$

in terms of the $r \times r$ diagonal matrices

$$\hat{f}(\varepsilon) = \begin{pmatrix} f_1(\varepsilon) & 0 & \cdots & 0 \\ 0 & f_2(\varepsilon) & \cdots & 0 \\ \vdots & \vdots & \ddots & \vdots \\ 0 & 0 & \cdots & f_r(\varepsilon) \end{pmatrix} \tag{68}$$

for the Bose-Einstein or Fermi-Dirac distributions of the reservoirs:

$$f_l(\varepsilon) = \frac{1}{\mathrm{e}^{\beta_l(\varepsilon - \mu_l)} - \theta} \,, \tag{69}$$

and $\hat{\lambda}_E = (\lambda_{lE}\, \delta_{ll'})$ and $\hat{\lambda}_N = (\lambda_{lN}\, \delta_{ll'})$ for the counting parameters.

Inserting into the definition (48) and using Eq. (66), the cumulant generating function is given for independent particles by

$$Q_{\mathbf{A}}(\boldsymbol{\lambda}) = \theta\, g_s \int \frac{d\varepsilon}{2\pi\hbar} \ln\det\left\{1 - \theta\hat{f}(\varepsilon)\left[\hat{S}^\dagger(\varepsilon)\,\mathrm{e}^{\varepsilon\hat{\lambda}_E+\hat{\lambda}_N}\,\hat{S}(\varepsilon)\,\mathrm{e}^{-\varepsilon\hat{\lambda}_E-\hat{\lambda}_N} - 1\right]\right\}. \tag{70}$$

The multivariate fluctuation relation (53) is satisfied. Here, the conservations of energy and particle number allow the currents to be defined with respect to some reference reservoir because the determinant inside the expression of the generating function is invariant under the transformations $\exp(\varepsilon\hat{\lambda}_E+\hat{\lambda}_N) \to \exp(\varepsilon\hat{\lambda}_E+\hat{\lambda}_N+\chi\,\hat{1})$ for any function $\chi(\varepsilon)$ of the energy ε and the identity matrix $\hat{1}$. For these systems, the multivariate fluctuation relation can be directly checked using the symmetry of the scattering matrix under time reversal [51]. Using Eqs. (49) and (50), the Landauer-Büttiker formulas for the particle and energy mean currents are recovered [8–22]. The diffusivities characterizing noise, as well as higher cumulants, can also be obtained. Moreover, the multivariate fluctuation relation (53) leads to a series of time-reversal symmetry relations between the response coefficients and the cumulants, including the Green-Kubo formulae and Onsager reciprocity relations. The advantage of the scattering approach is that these transport properties can be determined keeping the quantum coherence described by the scattering matrix $\hat{S}(\varepsilon)$.

B. Time asymmetry of temporal disorder and entropy production

Now, we turn to the characterization of dynamical randomness and thermodynamic entropy production in scattering and transport processes.

In the eighties, effort has been devoted to the extension of chaos theory to quantum systems. In particular, Connes, Narnhofer, and Thirring (CNT) [27, 28] has extended to quantum systems the concept of Kolmogorov-Sinai (KS) entropy per unit time [25, 26], which characterizes dynamical randomness, i.e., temporal disorder. It has been shown that quantum systems with a discrete energy spectrum have no dynamical randomness, as expected because their time evolution is quasiperiodic (with a finite number of incommensurate frequencies) or almost periodic (with countably many incommensurate frequencies). This is the case for the internal dynamics in the space of bound states. Yet, the CNT entropy per unit may be positive for infinite quantum systems at positive temperature and particle density. For such systems with independent particles, the expression of the CNT entropy has even been obtained [28], which is similar to the well-known formula of the thermodynamic entropy per unit volume for ideal gases of bosons or fermions [93]. However, the CNT entropy characterizes the temporal disorder, instead of the spatial disorder as the thermodynamic entropy does. The classical analogue of the CNT entropy is the KS entropy, this latter being infinite for ideal gases [94]. For this reason, it is required to keep a finite resolution ϵ in order to define the ϵ-entropy per unit time, which becomes infinite as $\epsilon \to 0$ [24, 36]. For classical ideal gases, the resolution is the volume of a one-body phase-space cell $\epsilon = \Delta x \Delta p$ and the ϵ-entropy per unit time is in correspondence with the CNT entropy under the usual condition $\Delta x \Delta p = 2\pi\hbar$ [95–97].

More recently, a fundamental relationship has been established between temporal disorder and the thermodynamic entropy production by introducing a time-reversed coentropy per unit time h^{R} besides the previously defined entropy per unit time h [29–33]. If the entropy per unit time measures temporal disorder by the rate of decay of path probabilities as the number of observations increases in time, the coentropy is defined as the rate of decay of the probability of the time-reversed paths. For Markovian stochastic processes as well as for effusion processes [29–33], the thermodynamic entropy production turns out to be given by the difference between the time-reversed coentropy and the entropy per unit time:

$$\frac{1}{k_{\mathrm{B}}}\frac{d_{\mathrm{i}}S}{dt} = h^{\mathrm{R}} - h \geq 0\,. \tag{71}$$

This difference forms a Kullback-Leibler divergence or relative entropy, which is known to be always non negative [98, 99], so that there is agreement with the second law of thermodynamics. In classical systems, both the entropy per unit time and its associated coentropy increases as $\ln(1/\epsilon)$ if the resolution decreases $\epsilon \to 0$. This behavior does not concern the thermodynamic entropy production because this latter is given by the difference (71), for which the terms with $\ln(1/\epsilon)$ cancel each other. We notice that the Kullback-Leibler divergence giving the thermodynamic entropy production has also been studied without considering the quantities h and h^{R} [40–42, 100].

Remarkably, Eq. (71) can be extended to quantum systems such as ideal gases of bosons or fermions flowing between reservoirs in a multiterminal circuit. Since ϵ may not take values smaller than the one fixed by Planck's constant, both the entropy per unit time h and its associated coentropy h^{R} take absolute values independent of the resolution and intrinsically determined by the quantum nature of the fundamental dynamics. The aim of this subsection is to show in detail how these ideas can be developed.

As shown in Fig. 1c, particles incoming from the channel a with their momentum between $p > 0$ and $p+\Delta p > 0$ may be scattered into the channel b with probability $|S_{ba}(\varepsilon)|^2$ at the energy (29). Their velocity is given by $|d\varepsilon/dp| = |p/m|$ so that they travel a distance $\Delta x_{\parallel} = t\,|d\varepsilon/dp|$ during the time interval $[0,t]$. In the incoming channel $a = l\mathbf{n}$, the number of possible one-body states (28) that can be occupied by a particle of momentum in the interval $[p, p+\Delta p]$ is given by

$$t\, g_s \left|\frac{d\varepsilon}{dp}\right| \frac{\Delta p}{2\pi\hbar}\,. \tag{72}$$

Since a fraction $|S_{ba}(\varepsilon)|^2$ is scattered into the channel $b = l'\mathbf{n}'$, the number of possible states following the path $\alpha = a \to b$ with momentum in $[p, p+\Delta p]$ can thus be evaluated per unit time to be equal to

$$\frac{dM_\alpha}{dt} = g_s \left|\frac{d\varepsilon}{dp}\right| \frac{\Delta p}{2\pi\hbar}\,|S_{ba}(\varepsilon)|^2\,. \tag{73}$$

In the channel $a = l\mathbf{n}$, these states have the mean occupation number $f_l(\varepsilon)$ of the incoming reservoir l.

During the time interval $[0,t]$, the one-body states of the path $\alpha = a \to b$ may accommodate a random number n of particles. Its probability distribution takes the form

$$P(n) = \frac{f^n}{(1+\theta\, f)^{n+\theta}} \tag{74}$$

where $\theta = +1$ and $n \in \{0,1,2,3,...\}$ for bosons, while $\theta = -1$ and $n \in \{0,1\}$ for fermions. The mean occupation number is recovered as $f = \langle n\rangle = \sum_n n\,P(n)$. The disorder among the particles following some path α is given by

$$-\sum_n P(n)\,\ln P(n) = -f\,\ln f + (f+\theta)\,\ln(1+\theta\, f)\,. \tag{75}$$

This disorder manifests itself in time at the rate (73) so that the entropy per unit time is obtained as

$$h = \sum_\alpha \frac{dM_\alpha}{dt}\left[-\sum_n P_\alpha(n)\,\ln P_\alpha(n)\right] \geq 0\,. \tag{76}$$

A time-reversed coentropy per unit time is defined by considering the time-reversed one-body paths $\alpha^{\rm R}$. These paths are weighted by the mean occupation number $f_{l'}$ of the reservoir l' corresponding to the outgoing channel $b = l'\mathbf{n}'$ of the forward path $\alpha = a \to b = l\mathbf{n} \to l'\mathbf{n}'$. Accordingly, the probability distribution $P^{\rm R}_\alpha(n)$ of the reversed path has the mean occupation number $f_{l'}$. The rate of decay in time of these probabilities defines the time-reversed coentropy per unit time

$$h^{\rm R} = \sum_\alpha \frac{dM_\alpha}{dt}\left[-\sum_n P_\alpha(n)\,\ln P^{\rm R}_\alpha(n)\right], \tag{77}$$

by averaging again over the forward process.

According to Eq. (71), the thermodynamic entropy production is thus given by

$$\frac{1}{k_{\rm B}}\frac{d_{\rm i}S}{dt} = h^{\rm R} - h = \sum_\alpha \frac{dM_\alpha}{dt}\,\sum_n P_\alpha(n)\,\ln\frac{P_\alpha(n)}{P^{\rm R}_\alpha(n)} \geq 0\,, \tag{78}$$

which is positive out of equilibrium and vanishes at equilibrium where $P_\alpha(n) = P^{\rm R}_\alpha(n)$.

The crucial point is that some particles are transmitted to a different reservoir, while others are reflected back into the same reservoir, from which they are coming out. For these latter particles, the mean occupation number is the same for the path α as for the time-reversed path $\alpha^{\rm R}$. This is no longer the case for the particles exchanged between two reservoirs at different temperatures or chemical potentials, for which $f_l \neq f_{l'}$. Now, the reflection and transmission coefficients are defined by

$$R_{aa}(\varepsilon) \;\equiv\; |S_{aa}(\varepsilon)|^2\,, \tag{79}$$

$$T_{ba}(\varepsilon) \;\equiv\; |S_{ba}(\varepsilon)|^2 \qquad \text{for} \quad a \neq b\,, \tag{80}$$

and they satisfy

$$R_{aa}(\varepsilon) + \sum_{b(\neq a)} T_{ba}(\varepsilon) = 1\,, \tag{81}$$

as the consequence of the unitarity of the scattering matrix. Therefore, only the paths $\alpha = a \to b$ between two different reservoirs contribute to the entropy production. For these paths, $|S_{ba}(\varepsilon)|^2 = T_{ba}(\varepsilon)$ in Eq. (73). Moreover, the mean occupation numbers satisfy

$$\frac{f_l}{1+\theta\, f_l} = \mathrm{e}^{-\beta_l(\varepsilon-\mu_l)}\,, \tag{82}$$

so that the standard expression of the thermodynamic entropy production is recovered from Eq. (71)

$$\frac{1}{k_{\rm B}}\frac{d_{\rm i}S}{dt} = h^{\rm R} - h = \sum_{l=1}^{r-1} \left(A_{lE}\,\langle J_{lE}\rangle_{\mathbf{A}} + A_{lN}\,\langle J_{lN}\rangle_{\mathbf{A}}\right), \tag{83}$$

in terms of the affinities (45)-(46) and the mean currents (49)-(50) [13–22]. This shows that thermodynamic entropy is produced due to time asymmetry in the temporal disorder of nonequilibrium processes.

The general results of the present Section III are applied to the transport of fermions and bosons in the next Sections IV and V.

IV. TRANSPORT OF FERMIONS

A. Generalities

We consider a two-terminal circuit as in Fig. 1b with a separable potential describing a harmonic transverse potential as in Eq. (26). The channels open at the energy thresholds

$$\varepsilon_{0n} = \hbar\omega\left(n+\frac{1}{2}\right) \qquad \text{with} \quad n = 0, 1, 2, 3, ... \tag{84}$$

As the one-body energy ε increases, the average number of open channels goes as $N_{\rm av}(\varepsilon) \simeq \varepsilon/(\hbar\omega)$ for such a circuit. For simplicity, the Pöschl-Teller barrier is replaced by the inverted parabolic barrier of Fig. 3c. Accordingly, the transmission probability in the $n^{\rm th}$ channel is given by

$$T_n(\varepsilon) = T(\varepsilon - \varepsilon_{0n})\,, \tag{85}$$

in terms of the function (32). In Fig. 4, the total transmission probability $\sum_n T_n(\varepsilon)$ is depicted as a function of the rescaled energy $\varepsilon/(\hbar\omega)$. Since the barrier culminates at v_0 and its width is small enough, the cumulated transmission probability increases by steps at the energies $\varepsilon = v_0 + \hbar\omega(n+1/2)$ with $n = 0, 1, 2, 3, ...$, as observed in Fig. 4. At low enough temperature, the Fermi-Dirac distribution also forms a step, which leads to the quantization of conductance.

The circuit is at equilibrium if the chemical potentials and temperatures of the left- and right-hand reservoirs are equal so that their Fermi-Dirac distributions are identical $f_{\rm L} = f_{\rm R} = f$. Close to this equilibrium, the conductance is given by Landauer-Büttiker formula

$$G = g_s \sum_{n=0}^{\infty} \int_{\varepsilon_{0n}}^{\infty} \frac{d\varepsilon}{2\pi\hbar}\, T_n(\varepsilon)\, \left(-\frac{\partial f}{\partial E}\right), \tag{86}$$

where $f = \left[\mathrm{e}^{\beta(\varepsilon-\mu)}+1\right]^{-1}$ is the common Fermi-Dirac distribution at the chemical potential μ and the inverse temperature β [3–8]. This conductance is shown in Fig. 5 at low enough temperature to manifest its quantization in terms of the universal conductance $G_0 = g_s/(2\pi\hbar)$. Nowadays, this phenomenon has been observed not only with electrons [101], but also with ultracold fermionic ^{6}Li atoms [55]. As the temperature increases, the quantization steps disappear and the conductance takes its average value $G_{\rm av} \simeq G_0(\mu - v_0)/(\hbar\omega)$ (dashed line in Fig. 5), which is independent of the temperature for given chemical potential μ.

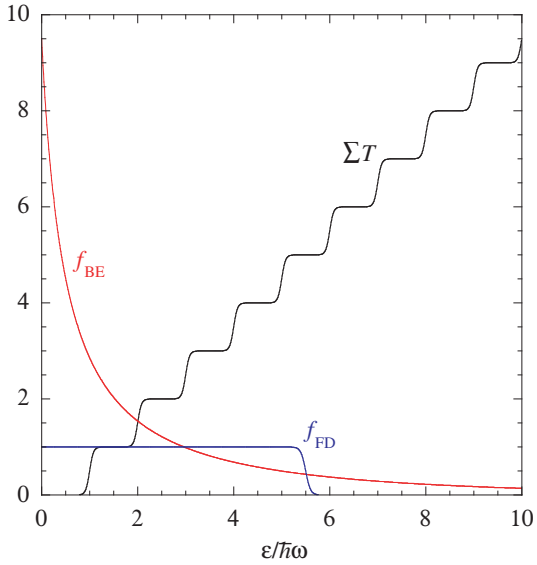

FIG. 4: The transmission probability $\sum T = \sum_n T_n(\varepsilon)$ versus the rescaled energy $\varepsilon/(\hbar\omega)$ for a two-terminal circuit of potential $u(x,y) = v(x) + m\omega^2 y^2/2$ formed by a harmonic waveguide and a constriction described by the inverted parabolic barrier $v(x) = v_0 - m\gamma^2 x^2/2$ with $v_0 = \hbar\omega/2$ and $\gamma/\omega = 0.25$ [82]. $f_{\rm FD}$ is the Fermi-Dirac distribution of rescaled chemical potential $\mu/(\hbar\omega) = 5.5$ and temperature $k_{\rm B}T/(\hbar\omega) = 0.05$. $f_{\rm BE}$ is the Bose-Einstein distribution of rescaled chemical potential $\mu/(\hbar\omega) = -0.5$ and temperature $k_{\rm B}T/(\hbar\omega) = 5$.

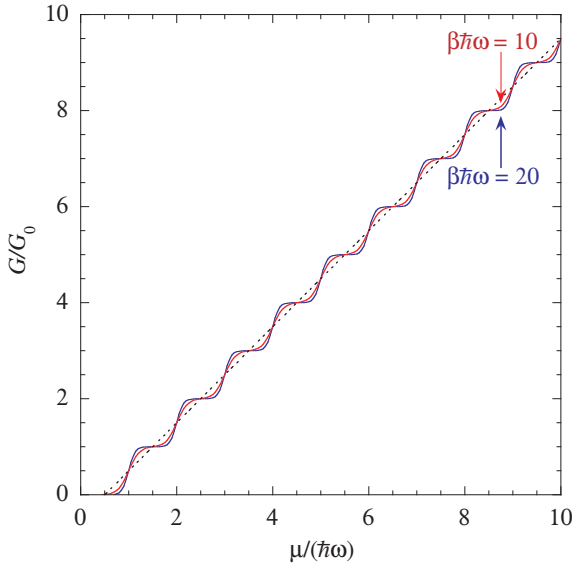

FIG. 5: The fermionic conductance (86) in units of the universal conductance $G_0 = g_s/(2\pi\hbar)$ versus the rescaled chemical potential $\mu/(\hbar\omega)$ for two different rescaled inverse temperatures $\beta\hbar\omega$ (solid lines). The dashed line depicts the average conductance $G_{\rm av}/G_0 \simeq (\mu - v_0)/(\hbar\omega)$.

B. Full counting statistics and multivariate fluctuation relation

Beyond conductance, transport fluctuations are characterized by their statistical cumulants. All the cumulants are captured in their generating function given in general by Eq. (70). For fermions with $\theta = -1$, the cumulant generating

function takes the form

$$Q_{\mathbf{A}}(\boldsymbol{\lambda}) = -g_s \int \frac{d\varepsilon}{2\pi\hbar} \ln\det\left\{1 + \hat{f}(\varepsilon)\left[\hat{S}^\dagger(\varepsilon)\,\mathrm{e}^{\varepsilon\hat{\lambda}_E+\hat{\lambda}_N}\,\hat{S}(\varepsilon)\,\mathrm{e}^{-\varepsilon\hat{\lambda}_E-\hat{\lambda}_N} - 1\right]\right\} , \tag{87}$$

which is equivalent to the Levitov-Lesovik formula [10, 11, 22, 51].

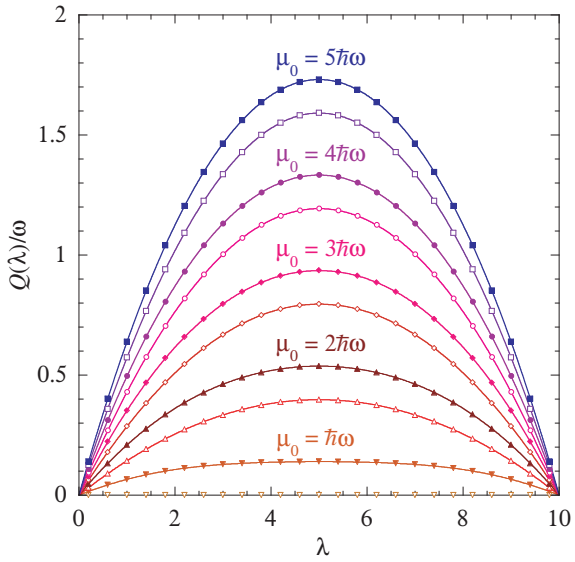

FIG. 6: Fermionic cumulant generating function (88) with $\lambda_E = 0$ versus the counting parameter $\lambda_N = \lambda$ for fermions flowing in the same two-terminal circuit as in Fig. 4 with the inverted parabolic barrier of parameters $v_0 = \hbar\omega/2$ and $\gamma/\omega = 0.25$. The rescaled inverse temperature is $\beta\hbar\omega = 20$. The chemical potentials of the left- and right-hand reservoirs are taken as $\mu_{\rm L} = \mu_0 + \hbar\omega/4$ and $\mu_{\rm R} = \mu_0 - \hbar\omega/4$ with $\mu_0/(\hbar\omega) = 0.5, 1, 1.5, 2, 2.5, 3, 3.5, 4, 4.5, 5$.

For the two-terminal circuit that we consider, the scattering matrix is provided by Eq. (31) so that the cumulant generating function becomes

$$Q_{\mathbf{A}}(\boldsymbol{\lambda}) = -g_s \sum_{n=0}^{\infty} \int_{\varepsilon_{0n}}^{\infty} \frac{d\varepsilon}{2\pi\hbar} \ln\left\{1 + T_n(\varepsilon)\left[f_{\rm L}(1-f_{\rm R})\left(\mathrm{e}^{-\varepsilon\lambda_E-\lambda_N} - 1\right) + f_{\rm R}(1-f_{\rm L})\left(\mathrm{e}^{\varepsilon\lambda_E+\lambda_N} - 1\right)\right]\right\} . \tag{88}$$

The multivariate fluctuation relation is satisfied:

$$Q_{\mathbf{A}}(\lambda_E, \lambda_N) = Q_{\mathbf{A}}(A_E - \lambda_E, A_N - \lambda_N) \tag{89}$$

with respect to the thermal and chemical affinities

$$A_E = \beta_{\rm R} - \beta_{\rm L} , \tag{90}$$

$$A_N = \beta_{\rm L}\,\mu_{\rm L} - \beta_{\rm R}\,\mu_{\rm R} . \tag{91}$$

The cumulant generating function (88) is depicted in Fig. 6 for the particle current in the two-terminal circuit described in Fig. 4 with the conductance of Fig. 5. The circuit is driven out of equilibrium by a bias in the chemical potentials of the two reservoirs so that the chemical affinity (91) takes the value $A_N = 10$. The thermal affinity (90) is vanishing because the temperature is uniform. The symmetry of the generating functions with respect to the reflection $\lambda_N \to A_N - \lambda_N$ is the expression of the fluctuation relation (89) with $A_E = 0$ and $\lambda_E = 0$. The slope of the generating function at $\lambda_N = \lambda = 0$ gives the average value of the particle current and the curvature its diffusivity. We observe that the mean current increases with $\mu_0 = (\mu_{\rm L} + \mu_{\rm R})/2$ because the bias is constant while the conductance increases as seen in Fig. 5. For $\mu_0 = 0.5\hbar\omega$, the conductance is tiny so that the generating function is flat in Fig. 6. The middle of the first step of conductance is reached for $\mu_0 = \hbar\omega$ so that the generating function now takes a non-negligible value. The generating function becomes higher and higher from step to step as $\mu_0/(\hbar\omega)$ continues to increase in Fig. 6. The time-reversal symmetry is always satisfied.

C. Temporal disorder

For ideal gases of fermions flowing in a two-terminal circuit, the CNT entropy per unit time (76) is given by

$$h = g_s \sum_{n=0}^{\infty} \int_{\varepsilon_{0n}}^{\infty} \frac{d\varepsilon}{2\pi\hbar} \left[-f_{\rm L} \ln f_{\rm L} - (1-f_{\rm L}) \ln(1-f_{\rm L}) - f_{\rm R} \ln f_{\rm R} - (1-f_{\rm R}) \ln(1-f_{\rm R}) \right] , \tag{92}$$

in terms of the Fermi-Dirac distributions $f_{\rm L}$ and $f_{\rm R}$ of the left- and right-hand reservoirs. The transmission probability has disappeared because the transmitted and reflected paths are both weighted by the mean occupation number of the same reservoirs, from which the particles are outgoing, so that the transmission and reflection probabilities sum to unity by the unitarity of the scattering matrix and Eq. (81). Besides, there is a flow of fermions coming from the left-hand reservoir and another one from the right-hand reservoir, which explains the presence of the corresponding terms in Eq. (92). The sum over the channels is still present because the flows between the reservoirs become larger and larger as the number of open channels increases with the chemical potential.

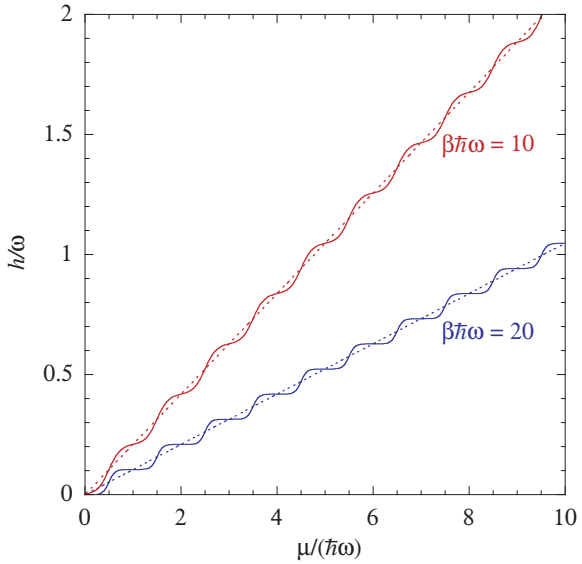

FIG. 7: The rescaled CNT entropy per unit time h/ω given by Eq. (93) versus the rescaled chemical potential $\mu/(\hbar\omega)$ for a fermionic ideal gas with $g_s = 2$ in the same two-terminal circuit as in Fig. 4 with the inverted parabolic barrier of parameters $v_0 = \hbar\omega/2$ and $\gamma/\omega = 0.25$ for two different rescaled inverse temperatures $\beta\hbar\omega = 10, 20$ (solid lines). The circuit is at equilibrium with uniform chemical potential and temperature. The dashed lines depict the average value (94) of the CNT entropy per unit time.

Now, if the circuit is at equilibrium with uniform temperature and chemical potential, the CNT entropy per unit time (92) reduces to

$$h = 2\, g_s \sum_{n=0}^{\infty} \int_{\varepsilon_{0n}}^{\infty} \frac{d\varepsilon}{2\pi\hbar} \left[-f \ln f - (1-f) \ln(1-f) \right] , \tag{93}$$

with $f = f_{\rm L} = f_{\rm R} = \left[{\rm e}^{\beta(\varepsilon-\mu)} + 1 \right]^{-1}$, which is shown in Fig. 7 for the two-terminal circuit of Fig. 4. We observe quantization steps as in the conductance in Fig. 5. However, the steps are not located at the energies $\varepsilon = v_0 + \varepsilon_{0n}$ of the top of the barrier in each open channel, but instead at the energies $\varepsilon = \varepsilon_{0n} = \hbar\omega(n+1/2)$ where the channels open (for $n = 0, 1, 2, 3, ...$).

Since the average number of open channels at the chemical potential μ is given by $N_{\rm av}(\mu) \simeq \mu/(\hbar\omega)$ in the two-terminal circuit, the average value of the CNT entropy can be evaluated as

$$h_{\rm av} \simeq g_s \frac{\pi k_{\rm B} T}{3\hbar} \frac{\mu}{\hbar\omega} . \tag{94}$$

Contrary to the conductance, the CNT entropy per unit time increases with the temperature. It vanishes as the temperature goes to zero, as it should because there is no disorder in a quantum gas at absolute zero [93].

At equilibrium, the CNT entropy per unit time is equal to the associated coentropy, $h = h^{\rm R}$. They differ out of equilibrium $h^{\rm R} > h$ and their difference gives the thermodynamic entropy production by Eq. (83).

V. TRANSPORT OF BOSONS

A. Generalities

The Bose-Einstein distribution $f_l = \left[\mathrm{e}^{\beta_l(\varepsilon-\mu_l)}-1\right]^{-1}$ diverges if the energy reaches the chemical potential $\varepsilon = \mu_l$, which corresponds to the condensation of bosons into the lowest energy level at low temperature. Transport of such condensates is a topic that is not treated here. Therefore, we assume that the chemical potential of every reservoir is always lower than the minimum possible energy: $\mu_l < \varepsilon_{00} = \hbar\omega/2$ for all $l = 1, 2, ..., r$. An example of such a Bose-Einstein distribution is shown in Fig. 4. If the temperature is low, the distribution is concentrated near the chemical potential so that few energy states are occupied in the open channels. Accordingly, the temperature should be increased to get a sufficiently large conductance. Contrary to the Fermi-Dirac distribution, the Bose-Einstein distribution is not step-like at low temperature so that, for bosons, the conductance does not manifest a phenomenon of quantization as for fermions.

B. Full counting statistics and multivariate fluctuation relation

With $\theta = +1$, Eq. (70) gives the cumulant generating function for bosons:

$$Q_{\mathbf{A}}(\boldsymbol{\lambda}) = +g_s \int \frac{d\varepsilon}{2\pi\hbar} \ln\det\left\{1 - \hat{f}(\varepsilon)\left[\hat{S}^\dagger(\varepsilon)\,\mathrm{e}^{\varepsilon\hat{\lambda}_E+\hat{\lambda}_N}\,\hat{S}(\varepsilon)\,\mathrm{e}^{-\varepsilon\hat{\lambda}_E-\hat{\lambda}_N} - 1\right]\right\}, \tag{95}$$

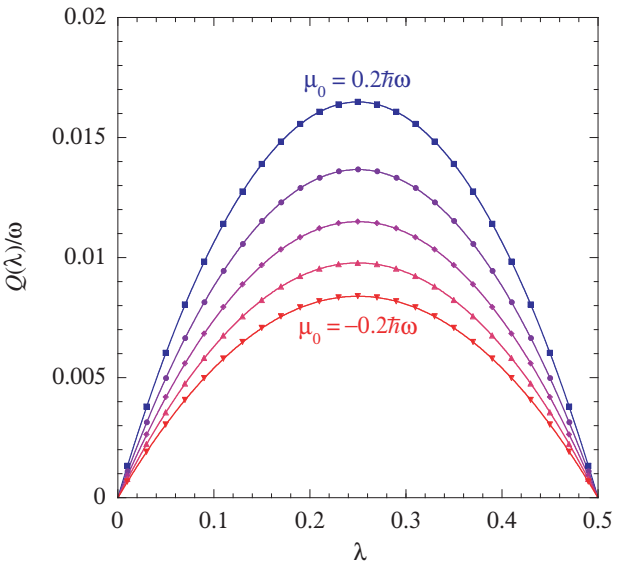

FIG. 8: Bosonic cumulant generating function (96) with $\lambda_E = 0$ versus the counting parameter $\lambda_N = \lambda$ for bosons flowing in the same two-terminal circuit as in Fig. 4 with the inverted parabolic barrier of parameters $v_0 = \hbar\omega/2$ and $\gamma/\omega = 0.25$. The rescaled inverse temperature is $\beta\hbar\omega = 1$. The chemical potentials of the left- and right-hand reservoirs are taken as $\mu_{\mathrm{L}} = \mu_0 + \hbar\omega/4$ and $\mu_{\mathrm{R}} = \mu_0 - \hbar\omega/4$ with $\mu_0/(\hbar\omega) = -0.2, -0.1, 0, 0.1, 0.2$.

For the two-terminal circuit with a constriction described by the scattering matrix (31) between reservoirs of Bose-Einstein distributions f_{L} and f_{R}, the cumulant generating function becomes

$$Q_{\mathbf{A}}(\boldsymbol{\lambda}) = g_s \sum_{n=0}^{\infty} \int_{\varepsilon_{0n}}^{\infty} \frac{d\varepsilon}{2\pi\hbar} \ln\left\{1 - T_n(\varepsilon)\left[f_{\mathrm{L}}(1+f_{\mathrm{R}})\left(\mathrm{e}^{-\varepsilon\lambda_E-\lambda_N}-1\right) + f_{\mathrm{R}}(1+f_{\mathrm{L}})\left(\mathrm{e}^{\varepsilon\lambda_E+\lambda_N}-1\right)\right]\right\}, \tag{96}$$

which also obeys the multivariate fluctuation relation (89) with respect to the affinities (90) and (91). This generating function is depicted in Fig. 8 for the full counting statistics of the particle current by taking a uniform temperature, but a positive chemical affinity $A_N = 0.5$ for different values of the mean chemical potential $\mu_0 = (\mu_{\mathrm{L}} + \mu_{\mathrm{R}})/2$ between both reservoirs. First of all, we observe the symmetry $\lambda_N \to A_N - \lambda_N$ of the fluctuation relation as a consequence of

microreversibility. Moreover, the generating function increases with μ_0 because the energy states are more and more occupied as the mean chemical potential μ_0 becomes larger. The slope at $\lambda_N = \lambda = 0$ increases and, thus, the mean current. For $\mu_0 = 0.2\hbar\omega$, the chemical potential of the left-hand reservoir $\mu_{\rm L} = \mu_0 + 0.25\hbar\omega$ is close to the threshold of the first channel at the energy $\varepsilon_{00} = 0.5\hbar\omega$, but without reaching it as required by the aforementioned condition to avoid the formation of a condensate.

C. Temporal disorder

For ideal gases of bosons in the two-terminal circuit, the CNT entropy per unit time (76) is given by

$$h = g_s \sum_{n=0}^{\infty} \int_{\varepsilon_{0n}}^{\infty} \frac{d\varepsilon}{2\pi\hbar} \left[-f_{\rm L} \ln f_{\rm L} + (1+f_{\rm L}) \ln(1+f_{\rm L}) - f_{\rm R} \ln f_{\rm R} + (1+f_{\rm R}) \ln(1+f_{\rm R}) \right] , \tag{97}$$

with the Bose-Einstein distributions $f_{\rm L}$ and $f_{\rm R}$ of the left- and right-hand reservoirs. Again, the CNT entropy per unit time does not depend on the transmission probability. As more and more channels are populated, the flows between the reservoirs become larger and larger.

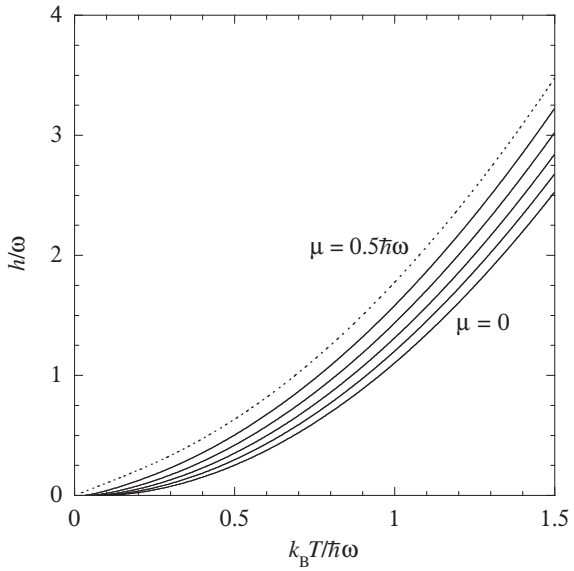

FIG. 9: The rescaled CNT entropy per unit time h/ω given by Eq. (98) versus the rescaled temperature $k_{\rm B}T/(\hbar\omega)$ for a bosonic ideal gas with $g_s = 1$ in the same two-terminal circuit as in Fig. 4 with the inverted parabolic barrier of parameters $v_0 = \hbar\omega/2$ and $\gamma/\omega = 0.25$ for different values of the rescaled chemical potential $\mu/(\hbar\omega) = 0, 0.1, 0.2, 0.3, 0.4$ (solid lines) and $\mu/(\hbar\omega) = 0.5$ (dashed line). The circuit is at equilibrium with uniform chemical potential and temperature.

At equilibrium with uniform temperature and chemical potential, the CNT entropy per unit time (97) is equal to

$$h = 2\, g_s \sum_{n=0}^{\infty} \int_{\varepsilon_{0n}}^{\infty} \frac{d\varepsilon}{2\pi\hbar} \left[-f \ln f + (1+f) \ln(1+f) \right] , \tag{98}$$

with $f = f_{\rm L} = f_{\rm R} = \left[{\rm e}^{\beta(\varepsilon-\mu)} - 1 \right]^{-1}$ and $\varepsilon_{0n} = \hbar\omega(n+1/2)$. This quantity characterizing temporal disorder is depicted in Fig. 9 as a function of temperature for the circuit of Fig. 4. The CNT entropy per unit time vanishes with the temperature, again because there is no disorder in the quantum gas at absolute zero. The disorder increases with temperature, as well as with the chemical potential.

Out of equilibrium, the time-reversed coentropy per unit time becomes larger than the CNT entropy $h^{\rm R} > h$ because the thermodynamic entropy production (83) is then positive.

VI. TRANSPORT IN THE CLASSICAL LIMIT

A. Full counting statistics and multivariate fluctuation relation

The transport of electrons or ultracold atoms through a constriction at low temperature is the quantum analogue of the effusion of a classical ideal gas through a small hole in a wall separating two reservoirs, which has been studied a century ago by Knudsen and others [62–64]. More recently, the multivariate fluctuation relation has been obtained for effusion and its consequences investigated [51, 102–104]. The question arises whether the cumulative generating function of effusion can be deduced in the classical limit from the quantum formula (70). Our aim is here to show that it is indeed the case.

We consider ballistic motion through a cylindrical waveguide between two reservoirs, as in Fig. 1d. The perpendicular section can have any shape of area A. The transverse classical motion can even be chaotic. The average number of transverse modes is given by

$$N_{\rm av}(\varepsilon) \simeq \int \frac{d\mathbf{x}_\perp d\mathbf{p}_\perp}{(2\pi\hbar)^2}\,\theta(\varepsilon - h^0_{\perp\rm cl})\,, \tag{99}$$

where $h^0_{\perp\rm cl}$ is the classical Hamiltonian ruling the transverse motion and $\theta(\varepsilon-\varepsilon')$ is Heaviside's step function. For a billiard with $h^0_{\perp\rm cl} = \mathbf{p}_\perp^2/(2m)$, we get

$$N_{\rm av}(\varepsilon) \simeq \frac{m}{2\pi\hbar^2}\,A\,\varepsilon\,, \tag{100}$$

where m is the particle mass.

The fugacity in the $l^{\rm th}$ reservoir at the temperature T_l and chemical potential μ_l can be expressed as

$$\mathrm{e}^{\beta_l\mu_l} = \frac{1}{g_s}\left(\frac{2\pi\hbar^2}{mk_{\rm B}T_l}\right)^{3/2} n_l \tag{101}$$

in terms of the particle density n_l [93]. In the classical limit, the fugacities thus become much smaller than unity $\mathrm{e}^{\beta_l\mu_l} \ll 1$, so that the mean occupation numbers of both bosons and fermions can be approximated by Boltzmann's distributions:

$$f_l \simeq \mathrm{e}^{\beta_l\mu_l}\,\mathrm{e}^{-\beta_l\varepsilon}\,. \tag{102}$$

Moreover, the transmission probability through an open channel tends to the unit value in the classical limit, $T_n(\varepsilon) \simeq 1$. Consequently, both Eqs. (88) and (96) reduce to

$$Q_{\mathbf{A}}(\boldsymbol{\lambda}) \simeq \int_0^\infty d\varepsilon\,\left[w_{\rm L}(\varepsilon)\left(1-\mathrm{e}^{-\varepsilon\lambda_E-\lambda_N}\right) + w_{\rm R}(\varepsilon)\left(1-\mathrm{e}^{\varepsilon\lambda_E+\lambda_N}\right)\right]\,, \tag{103}$$

with the rates

$$w_l(\varepsilon) = \frac{A\,n_l}{\sqrt{2\pi mk_{\rm B}T_l}}\,\frac{\varepsilon}{k_{\rm B}T_l}\,\exp\left(-\frac{\varepsilon}{k_{\rm B}T_l}\right) \qquad \text{for} \quad l = {\rm L},{\rm R}\,, \tag{104}$$

which is indeed the expression of the cumulant generating function for the effusion of a classical gas through a small hole of area A [51, 102–104].

Since the ratio of the rates (104) has the following form

$$\frac{w_{\rm L}(\varepsilon)}{w_{\rm R}(\varepsilon)} = \mathrm{e}^{\varepsilon A_E + A_N} \tag{105}$$

in terms of the thermal and chemical affinities (90)-(91), the validity of the multivariate fluctuation relation (89) is confirmed.

B. Temporal disorder

Classically, the entropy per unit time can be evaluated by considering a fictitious surface Σ perpendicular to the cylindrical duct of sectional area A. The position, momentum, and spin components of every particle crossing this

surface are detected with a resolution $\Delta^3x\Delta^3p$. The number of particles detected by the cell $[\mathbf{x}_i, \mathbf{x}_i + \Delta\mathbf{x}]$ with the momentum $[\mathbf{p}_i, \mathbf{p}_i + \Delta\mathbf{p}]$ and its spin component $\sigma = -s, -s+1, ..., s-1, s$ during the time interval $[0, t]$ is equal to

$$N_{i\sigma} = \frac{1}{g_s} \left|\frac{p_{xi}}{m}\right| t\, A\, F_l(\mathbf{p}_i)\, \Delta^3 p\,, \tag{106}$$

where

$$F_l(\mathbf{p}) = \frac{n_l}{(2\pi m k_{\rm B} T_l)^{3/2}} \exp\left(-\frac{\mathbf{p}^2}{2mk_{\rm B}T_l}\right), \tag{107}$$

is the Maxwell distribution function at the temperature T_l and particle density n_l. The cylindrical hole being oriented in the x-direction, the Maxwell distribution should correspond to the left-hand reservoir $l = {\rm L}$ if $p_x > 0$ and to the right-hand reservoir $l = {\rm R}$ if $p_x < 0$. These $N_{i\sigma}$ particles are distributed uniformly in space inside the volume $|p_{xi}/m|\, t\, A$. If space is discretized into cells of volume $\Delta^3 x$, the number of different available positions is given by

$$M_i = \left|\frac{p_{xi}}{m}\right| \frac{t\, A}{\Delta^3 x}\,. \tag{108}$$

The entropy per unit time is calculated as the growth rate of the number of possible configurations for the $N_{i\sigma}$ particles among the M_i positions during the time interval $[0, t]$ [95–97]

$$h = \lim_{t\to\infty} \frac{1}{t} \ln \prod_{i,\sigma} \frac{M_i^{N_{i\sigma}}}{N_{i\sigma}!}\,. \tag{109}$$

Using Eqs. (106)-(108) and Stirling's formula, we obtain

$$h = A \int_{p_x>0} d^3p \left|\frac{p_x}{m}\right| F_{\rm L}(\mathbf{p}) \ln \frac{{\rm e}\, g_s}{F_{\rm L}(\mathbf{p})\, \Delta^3 x\, \Delta^3 p} + A \int_{p_x<0} d^3p \left|\frac{p_x}{m}\right| F_{\rm R}(\mathbf{p}) \ln \frac{{\rm e}\, g_s}{F_{\rm R}(\mathbf{p})\, \Delta^3 x\, \Delta^3 p}\,, \tag{110}$$

in terms of the Maxwell distribution functions (107) of the left- and right-hand reservoirs. This classical expression increases without bound as the phase-space resolution decreases, $\Delta^3x\Delta^3p \to 0$, since there is no limit to this resolution in classical physics.

Let us compare with the classical limit of the CNT entropy per unit time

$$h = g_s \sum_{n=0}^{\infty} \int_{\varepsilon_{0n}}^{\infty} \frac{d\varepsilon}{2\pi\hbar} \left[-f_{\rm L} \ln f_{\rm L} + (f_{\rm L} + \theta) \ln(1 + \theta\, f_{\rm L}) - f_{\rm R} \ln f_{\rm R} + (f_{\rm R} + \theta) \ln(1 + \theta\, f_{\rm R})\right], \tag{111}$$

for a flow between two reservoirs. In this limit where ${\rm e}^{\beta_l \mu_l} \ll 1$, the Bose-Einstein and Fermi-Dirac mean occupation numbers reduce to the Boltzmannian distribution (102), which can be expressed in terms of the Maxwellian distribution function (107) as follows:

$$f_l(\varepsilon) \simeq \frac{1}{g_s} F_l(\mathbf{p})\, (2\pi\hbar)^3\,, \tag{112}$$

at the energy $\varepsilon = \mathbf{p}^2/(2m)$. If ${\rm e}^{\beta_l \mu_l} \ll 1$, we find that $(f_l + \theta)\ln(1 + \theta\, f_l) = f_l + O(f_l^2)$. Using the average number of open channels given by Eq. (100), we indeed recover the classical expression (110) but with $\Delta^3x\Delta^3p = (2\pi\hbar)^3$, which is the phase-space volume occupied by one quantum state, as it should. The temporal disorder thus finds an absolute value in quantum mechanics and there is a neat correspondence of concepts.

The time-reversed coentropy per unit time can be treated similarly and its difference with respect to the entropy per unit time gives the thermodynamic entropy production (83).

VII. CONCLUSIONS

In the present paper, scattering theory is complemented by recent results on full counting statistics, the multivariate fluctuation relation, and temporal disorder, in order to establish relationships with thermodynamics.

On the one hand, statistics can be performed on repeated scattering events such as collisions between a finite set of particles, and theory aims at predicting the probabilities of the outcomes. On the other hand, the scattering events may happen continuously at certain rates determined by stationary particle flows from reservoirs. The latter

situation is described by many-body quantum mechanics since the number of particles varies, leading to full counting statistics, although standard scattering theory is described by quantum mechanics with a finite number of particles. Furthermore, energy should be continuously supplied to maintain stationary particle flows across an open system in contact with reservoirs so that transport processes dissipate energy, produce entropy, and, thus, generate irreversibility.

The present paper shows the unity of knowledge from scattering theory to thermodynamics, and from classical effusion to quantum transport for bosons and fermions.

The effusion of gases through a small hole – which has been studied a century ago by Knudsen and others [62] – is one of the simplest processes of kinetic theory [63, 64]. Nowadays, modern technology allows us to study the quantum analogues of effusion, i.e., the quantum transport of electrons in mesoscopic circuits at low temperatures [5, 101] and of ultracold atoms through a constriction formed in an optical trap [55]. In such transport processes, the motion is approximately ballistic and the circuit or the constriction can be treated with one-body scattering theory. The scattering events happen at some rate due to the contact with reservoirs at different chemical potentials or temperatures. In the present paper, we see for bosons and fermions how it is possible to use scattering theory to obtain the full counting statistics of the particle and energy currents, as well as the thermodynamic entropy production, while keeping the quantum coherence of one-body motion in the circuit or constriction. In particular, the Landauer-Büttiker formula for conductance is recovered thanks to the scattering approach.

The microreversibility of Hamiltonian quantum dynamics implies a fundamental symmetry in the full counting statistics, known as the multivariate fluctuation relation for currents. The validity of this relation is explicitly demonstrated for both bosons and fermions, flowing in a two-terminal circuit with a constriction. The multivariate fluctuation relation has fundamental implications on the linear and nonlinear response coefficients and the symmetry they may have as the consequence of microreversibility. In particular, generalizations of the Onsager reciprocity relations can be deduced from the multivariate fluctuation relation. Some of these implications have been tested experimentally for quantum electron transport, showing the importance of such results to understand irreversibility at the nanoscale [105–108]. We notice that the multivariate fluctuation relation is more powerful than the fluctuation relation for a single current because the multivariate relation can describe the coupling between several currents, such as the currents in a quantum point contact monitoring a double quantum dot, or the coupling between electric and heat currents. The multivariate fluctuation relation can be extended to systems subjected to an external magnetic field, in which circumstances the time-reversal symmetry only holds if we compare systems with opposite magnetic fields, $\mathbf{B}$ and $-\mathbf{B}$ [50, 53]. In these systems, the multivariate fluctuation relation has important consequences on the galvanomagnetic and thermomagnetic transport properties [51], which have not yet been explored in the nonlinear regimes.

Besides, another fundamental relationship is used to obtain the thermodynamic entropy production from the time asymmetry in the temporal disorder of the quantum gas flowing across the open system. Such a relationship is known since 2004 for stochastic Markovian processes [29], but its extension to quantum systems has been challenging. The temporal disorder is measured by the so-called Connes-Narnhofer-Thirring (CNT) entropy per unit time [27], a concept introduced in the eighties for the study of quantum chaos [109]. Recently, an associated time-reversed coentropy per unit time has been defined to characterize time asymmetry in the temporal disorder under nonequilibrium conditions [29–33]. The remarkable result is that the difference between the coentropy and the CNT entropy per unit time gives the thermodynamic entropy production for quantum systems as well. This result is here demonstrated from scattering theory for both bosonic and fermionic ideal gases. The CNT entropy per unit time is calculated for these quantum gases in a two-terminal circuit. For a fermionic gas, the CNT entropy per unit time manifests an effect of quantization similar to the one known for conductance. The CNT entropy per unit time vanishes at zero temperature where disorder no longer exists. Moreover, the temporal disorder takes an absolute value in quantum ideal gases because quantum mechanics imposes a fundamental limit determined by Planck's constant on the resolution in the measurement of canonically conjugated variables $\Delta x \Delta p = 2\pi\hbar$ or $\Delta t \Delta\varepsilon = 2\pi\hbar$. Such limits do not exist for classical variables so that the temporal disorder may take arbitrarily large values, as recognized long ago [24]. In quantum systems, this is no longer the case and an absolute value can be attributed to the temporal disorder and its time reversal. In this way, the thermodynamic entropy production can be related to time asymmetry in the temporal disorder characterized by the CNT entropy per unit time. These results represent the accomplishment of a series of advances since the eighties in the understanding of chaos and its consequences in quantum systems.

Many questions are open concerning the extension of these results beyond the ideal quantum gases of bosons and fermions considered in the present paper.

First, similar considerations apply to ultracold molecules moving in circuit-like potentials and possibly reacting. Mass separation can be envisaged in mixtures of quantum gases besides the coupling between the particle and thermal currents. A fascinating topic of great interest is the transport of quantum condensates in superconducting, superfluid, and topological quantum phases.

Interaction between the particles can be taken into account with the scattering and other approaches. For instance, electrons moving in two capacitively coupled circuits undergo Coulomb interactions, which can be described by two-body scattering theory, keeping the quantum coherence of the process.

Otherwise, quantum kinetic equations can be used such as the Uehling-Uhlenbeck equation [110], which is the analogue of Boltzmann kinetic equation for bosons or fermions, especially in their stochastic version. Indeed, the multivariate fluctuation relation has already been proved for the fluctuating Boltzmann equation ruling diluted or rarefied classical gases of interacting particles [111]. In such gases, the thermodynamic entropy production can be evaluated thanks to the H-theorem, obeyed by these kinetic equations. A challenge is to include quantum coherence, for instance by coupling the kinetic equation describing the thermal cloud to the nonlinear Schrödinger equation describing the condensate.

At the frontier between quantum and classical mechanics, the multiplication of quantum states adds a further level of complexity. This issue is addressed with random matrix theory and the semiclassical approach. Supposing that the scattering matrix is represented by a unitary random matrix, how will the cumulant generating function (70) behave for bosons or fermions? In this regard, we may wonder if signatures of this complexity will manifest themselves as corrections beyond the classical cumulant generating function (103), in particular, for classically chaotic scatterers. We hope to report on these fundamental questions in the future.

Acknowledgments

This research is financially supported by the Université Libre de Bruxelles and the Belgian Science Policy Office under the Interuniversity Attraction Pole project P7/18 "DYGEST".

[1] C. J. Joachain, *Quantum Collision Theory* (North-Holland, Amsterdam, 1975).
[2] J. R. Taylor, *Scattering Theory* (Dover, Mineola, 2000).
[3] S. Datta, *Electronic Transport in Mesoscopic Systems* (Cambridge University Press, Cambridge UK, 1995).
[4] Y. Imry, *Introduction to Mesoscopic Physics* (Oxford University Press, New York, 1997).
[5] D. K. Ferry, S. M. Goodnick, and J. Bird, *Transport in Nanostructures*, 2nd Edition (Cambridge University Press, Cambridge UK, 2009).
[6] Y. V. Nazarov and Y. M. Blanter, *Quantum Transport* (Cambridge University Press, Cambridge UK, 2009).
[7] R. Landauer, IBM J. Res. Develop. **1**, 223 (1957).
[8] M. Büttiker, Y. Imry, R. Landauer, and S. Pinhas, Phys. Rev. B **31**, 6207 (1985).
[9] U. Sivan and Y. Imry, Phys. Rev. B **33**, 551 (1986).
[10] L. S. Levitov and G. B. Lesovik, JETP Lett. **58**, 230 (1993).
[11] L. S. Levitov, H. W. Lee, and G. B. Lesovik, J. Math. Phys. **37**, 4845 (1996).
[12] Y. M. Blanter and M. Büttiker, Phys. Rep. **336**, 1 (2000).
[13] S. Tasaki, Chaos, Solitons & Fractals **12**, 2657 (2001).
[14] S. Tasaki and T. Matsui, in: L. Accardi and S. Tasaki, Editors, *Fundamental Aspects of Quantum Physics* (World Scientific, New Jersey, 2003) pp. 100-119.
[15] S. Tasaki and J. Takahashi, Prog. Theor. Phys. Suppl. **165**, 57 (2006).
[16] V. Jakšić and C.-A. Pillet, Commun. Math. Phys. **217**, 285 (2001).
[17] V. Jakšić and C.-A. Pillet, J. Stat. Phys. **108**, 787 (2002).
[18] W. Aschbacher, V. Jakšić, Y. Pautrat, and C.-A. Pillet, J. Math. Phys. **48**, 032101 (2007).
[19] L. Bruneau, V. Jakšić, and C.-A. Pillet, Commun. Math. Phys. **319**, 501(2013).
[20] V. Jakšić, Y. Ogata, Y. Pautrat, and C.-A. Pillet, in: J. Frohlich, M. Salmhofer, V. Mastropietro, W. De Roeck, and L. F. Cugliandolo, *Quantum Theory from Small to Large Scales* (Oxford, University Press, Oxford, 2012) pp. 213-410.
[21] V. Jakšić, B. Landon, and C.-A. Pillet, Ann. Henri Poincaré **14**, 1775 (2013).
[22] R. Ben Sâad and C.-A. Pillet, J. Math. Phys. **55**, 075202 (2014).
[23] J.-P. Eckmann and D. Ruelle, Rev. Mod. Phys. **57**, 617 (1985).
[24] P. Gaspard and X.-J. Wang, Phys. Rep. **235**, 291 (1993).
[25] A. N. Kolmogorov, Dokl. Akad. Nauk SSSR **124**, 754 (1959).
[26] Ya. G. Sinai, Dokl. Akad. Nauk SSSR **124**, 768 (1959).
[27] A. Connes, H. Narnhofer, and W. Thirring, Commun. Math. Phys. **112**, 691 (1987).
[28] H. Narnhofer and W. Thirring, Lett. Math. Phys. **14**, 89 (1987).
[29] P. Gaspard, J. Stat. Phys. **117**, 599 (2004).
[30] P. Gaspard, New J. Phys. **7**, 77 (2005).
[31] D. Andrieux, P. Gaspard, S. Ciliberto, N. Garnier, S. Joubaud, and A. Petrosyan, Phys. Rev. Lett. **98**, 150601 (2007).
[32] D. Andrieux, P. Gaspard, S. Ciliberto, N. Garnier, S. Joubaud, and A. Petrosyan, J. Stat. Mech. P01002 (2008).
[33] P. Gaspard, J. Math. Phys. **55**, 075208 (2014).
[34] P. Gaspard and G. Nicolis, Phys. Rev. Lett. **65**, 1693 (1990).
[35] J. R. Dorfman and P. Gaspard, Phys. Rev. E **51**, 28 (1995).

[36] P. Gaspard, *Chaos, Scattering and Statistical Mechanics* (Cambridge University Press, Cambridge UK, 1998).
[37] D. J. Evans, E. G. D. Cohen, and G. P. Morriss, Phys. Rev. Lett. **71**, 2401 (1993).
[38] G. Gallavotti, Phys. Rev. Lett. **77**, 4334 (1996).
[39] J. Kurchan, J. Phys. A: Math. Gen. **31**, 3719 (1998).
[40] J. L. Lebowitz and H. Spohn, J. Stat. Phys. **95**, 333 (1999).
[41] C. Maes, J. Stat. Phys. **95**, 367 (1999).
[42] C. Maes and K. Netočný, J. Stat. Phys. **110**, 269 (2003).
[43] M. Esposito, U. Harbola, and S. Mukamel, Rev. Mod. Phys. **81**, 1665 (2009).
[44] M. Campisi, P. Hänggi, and P. Talkner, Rev. Mod. Phys. **83**, 771 (2011); *Erratum*, *ibid.* **83**, 1653 (2011).
[45] U. Seifert, Rep. Prog. Phys. **75**, 126001 (2012).
[46] D. Andrieux and P. Gaspard, J. Chem. Phys. **121**, 6167 (2004).
[47] D. Andrieux and P. Gaspard, J. Stat. Mech. P01011 (2006).
[48] D. Andrieux and P. Gaspard, J. Stat. Mech. P02006 (2007).
[49] D. Andrieux and P. Gaspard, J. Stat. Phys. **127**, 107 (2007).
[50] D. Andrieux, P. Gaspard, T. Monnai, and S. Tasaki, New J. Phys. **11**, 043014 (2009); *Erratum*, *ibid.* **11**, 109802 (2009).
[51] P. Gaspard, New J. Phys. **15**, 115014 (2013).
[52] J. Tobiska and Yu. V. Nazarov, Phys. Rev. B **72**, 235328 (2005).
[53] K. Saito and Y. Utsumi, Phys. Rev. B **78**, 115429 (2008).
[54] J.-P. Brantut, C. Grenier, J. Meineke, D. Stadler, S. Krinner, C. Kollath, T. Esslinger, and A. Georges, Science **342**, 713 (2013).
[55] S. Krinner, D. Stadler, D. Husmann, J.-P. Brantut, and T. Esslinger, Nature **517**, 64 (2015).
[56] I. Burghardt and P. Gaspard, J. Chem. Phys. **100**, 6395 (1994).
[57] L. D. Landau and E. M. Lifshitz, *Quantum Mechanics* (Pergamon Press, Oxford, 1977).
[58] R. Folman, P. Krüger, D. Cassettari, B. Hessmo, T. Maier, and J. Schmiedmayer, Phys. Rev. Lett. **84**, 4749 (2000).
[59] R. Sánchez, R. López, D. Sánchez, and M. Büttiker, Phys. Rev. Lett. **104**, 076801 (2010).
[60] G. Bulnes Cuetara, M. Esposito, and P. Gaspard, Phys. Rev. B **84**, 165114 (2011).
[61] G. Bulnes Cuetara, M. Esposito, G. Schaller, and P. Gaspard, Phys. Rev. B **88**, 115134 (2013).
[62] M. Knudsen, Ann. d. Physik **28**, 999 (1909).
[63] R. D. Present, *Kinetic Theory of Gases* (McGraw-Hill, New York, 1958).
[64] R. K. Pathria, *Statistical Mechanics* (Pergamon, Oxford, 1972).
[65] C. Cohen-Tannoudji, B. Diu, and F. Laloë, *Quantum Mechanics* (Wiley, New York, 2006).
[66] E. P. Wigner, Phys. Rev. **98**, 145 (1955).
[67] H. Narnhofer and W. Thirring, Phys. Rev. A **23**, 1688 (1981).
[68] R. Balian and C. Bloch, Ann. Phys. **85**, 514 (1974).
[69] M. C. Gutzwiller, *Chaos in Classical and Quantum Mechanics* (Springer, New York, 1990).
[70] A. Voros, J. Phys. A: Math. Gen. **21**, 685 (1988).
[71] M. Pollicott, Invent. Math. **81**, 413 (1985).
[72] D. Ruelle, Phys. Rev. Lett. **56**, 405 (1986).
[73] D. Ruelle, J. Stat. Phys. **44**, 281 (1986).
[74] P. Gaspard, Scholarpedia **9**, 9806 (2014).
[75] P. Gaspard and S. A. Rice, J. Chem. Phys. **90** 2225 (1989).
[76] P. Gaspard and S. A. Rice, J. Chem. Phys. **90** 2242 (1989).
[77] P. Gaspard and S. A. Rice, J. Chem. Phys. **90** 2255 (1989).
[78] P. Gaspard, D. Alonso, T. Okuda, and K. Nakamura, Phys. Rev. E **50**, 2591 (1994).
[79] F. Barra and P. Gaspard, Phys. Rev. E **65**, 016205 (2001).
[80] F. Haake, *Quantum Signatures of Chaos*, 2nd Edition (Springer, Berlin, 2001).
[81] J. Rammer, *Quantum Field Theory of Non-equilibrium States* (Cambridge University Press, Cambridge UK, 2007).
[82] M. Büttiker, Phys. Rev. B **41**, 7906 (1990).
[83] U. Smilansky, in: E. Akkermans, G. Montambaux, J.-L. Pichard, and J. Zinn-Justin, Editors, *Mesoscopic Quantum Physics* (Elsevier, Amsterdam, 1995) pp. 373-433.
[84] K. Nakamura and T. Harayama, *Quantum Chaos and Quantum Dots* (Oxford University Press, Oxford, 2004).
[85] L. Onsager, Phys. Rev. **37**, 405 (1931).
[86] T. De Donder and P. Van Rysselberghe, *Affinity* (Stanford University Press, Menlo Park CA, 1936).
[87] I. Prigogine, *Introduction to Thermodynamics of Irreversible Processes* (Wiley, New York, 1967).
[88] S. R. de Groot and P. Mazur, *Non-Equilibrium Thermodynamics* (Dover, New York, 1984).
[89] H. B. Callen, *Thermodynamics and an Introduction to Thermostatistics* (Wiley, New-York, 1985).
[90] I. Klich, in: Y. V. Nazarov, Editor, *Quantum Noise in Mesoscopic Physics* (Kluwer, Dordrecht, 2003).
[91] J. E. Avron, S. Bachmann, G. M. Graff, and I. Klich, Commun. Math. Phys. **280**, 807 (2008).
[92] P. Gaspard, in: R. Klages, W. Just, and C. Jarzynski, Editors, *Nonequilibrium Statistical Physics of Small Systems: Fluctuation Relations and Beyond* (Wiley-VCH Verlag, Weinheim, 2013) pp. 213-257.
[93] K. Huang, *Statistical Mechanics* (Wiley, New York, 1963).
[94] I. P. Cornfeld, S. V. Fomin, and Ya. G. Sinai, *Ergodic Theory* (Springer-Verlag, New York, 1982).
[95] P. Gaspard, in: H. A. Cerdeira, R. Ramaswamy, M. C. Gutzwiller, and G. Casati, Editors, *Quantum Chaos* (World Scientific, Singapore, 1991) pp. 348-370.

[96] P. Gaspard, in: P. Cvitanović, I. Percival, and A. Wirzba, Editors, *Quantum Chaos - Quantum Measurement* (Kluwer, Dordrecht, 1992) pp. 19-42.
[97] P. Gaspard, Prog. Theor. Phys. Suppl. **116**, 369 (1994).
[98] A. Wehrl, Rev. Mod. Phys. **50**, 221 (1978).
[99] T. M. Cover and J. A. Thomas, *Elements of Information Theory*, 2nd edition (Wiley, Hoboken, 2006).
[100] I. Callens, W. De Roeck, T. Jacobs, C. Maes, and K. Netočný, Physica D **187**, 383 (2004).
[101] B. J. van Wees, H. van Houten, C. W. J. Beenakker, J. G. Williamson, L. P. Kouwenhoven, D. van der Marel, and C. T. Foxon, Phys. Rev. Lett. **60**, 848 (1988).
[102] B. Cleuren, C. Van den Broeck, and R. Kawai, Phys. Rev. E **74**, 021117 (2006).
[103] P. Gaspard and D. Andrieux, J. Stat. Mech. P03024 (2011).
[104] P. Gaspard, Acta Phys. Polon. B **44**, 815 (2013).
[105] Y. Utsumi, D. S. Golubev, M. Marthaler, K. Saito, T. Fujisawa, and G. Schön, Phys. Rev. B **81**, 125331 (2010).
[106] S. Nakamura, Y. Yamauchi, M. Hashisaka, K. Chida, K. Kobayashi, T. Ono, R. Leturcq, K. Ensslin, K. Saito, Y. Utsumi, and A. C. Gossard, Phys. Rev. Lett. **104**, 080602 (2010).
[107] S. Nakamura, Y. Yamauchi, M. Hashisaka, K. Chida, K. Kobayashi, T. Ono, R. Leturcq, K. Ensslin, K. Saito, Y. Utsumi, and A. C. Gossard, Phys. Rev. B **83**, 155431 (2011).
[108] B. Küng, C. Rössler, M. Beck, M. Marthaler, D. S. Golubev, Y. Utsumi, T. Ihn, and K. Ensslin, Phys. Rev. X **2**, 011001 (2012).
[109] F. Benatti, T. Hudetz, and A. Knauf, Commun. Math. Phys. **198**, 607 (1998).
[110] R. Balescu, *Equilibrium and Nonequilibrium Statistical Mechanics* (Wiley, New York, 1975).
[111] P. Gaspard, Physica A **392**, 639 (2013).